# Effects of fluorine substitution on the intermolecular interactions, energetics and packing behaviour of N-benzyl substituted diketopyrrolopyrroles

*Jesus Calvo-Castro,*[c] Graeme Morris,[a] Alan R. Kennedy,[b] and Callum J. McHugh*[a]*

[a] *School of Science and Sport, University of the West of Scotland, Paisley, PA1 2BE, UK.*
[b] *Department of Pure & Applied Chemistry, University of Strathclyde, Glasgow, G1 1XL, UK.*
[c] *School of Life and Medical Sciences, University of Hertfordshire, Hatfield, AL10 9AB, UK.*

**ABSTRACT:** Four novel systematically fluorinated DPPs and their single crystal structures are reported. Structures involving direct fluorination of the DPP core phenyl rings and N-benzyl groups, display 1-dimentional π-π stacking motifs; a characteristic of N-benzyl substitution, where long and short molecular axis displacement is induced by isosteric substitution of phenylic hydrogen atoms for fluorine atoms. This characteristic stacking behaviour is destroyed upon trifluoromethyl substitution at the para position of the core phenyl rings, in one case affording a novel molecular conformation and π-π dimer pair exhibiting a higher intermolecular interaction energy than any other structurally analogous DPP based system reported previously. This crystal structure also exhibits a unique orthogonal association of the π-π dimer pairs along the crystallographic *a* and *b* axes, resulting in the formation of a framework that is characterised by well-defined channels perpetuating along the length of the crystallographic *c* axis. The role of fluorine induced stabilisation and its impact on optoelectronic properties in these systems is identified via analysis of computed intermolecular interactions for all the crystal extracted nearest neighbour dimer pairs and their associated cropped equivalents. Our results clearly reinforce the positive role of benzyl substitution in DPP crystal structures to enhance optoelectronic behaviour. More importantly they demonstrate the significant impact small changes in molecular structure can have on the solid state properties of this molecular motif, particularly when fluorination is involved.

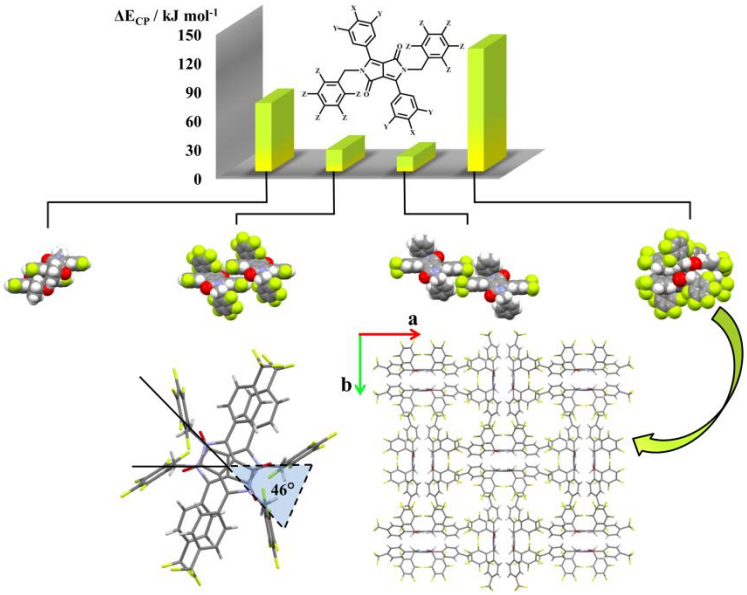


Dr. C. J. McHugh*
University of the West of Scotland
School of Science and Sport
Paisley, UK
PA1 2BE
Tel: +44 (141) 848 3210
Email: callum.mchugh@uws.ac.uk

# Effects of fluorine substitution on the intermolecular interactions, energetics and packing behaviour of N-benzyl substituted diketopyrrolopyrroles

*Jesus Calvo-Castro,*[c] Graeme Morris,[a] Alan R. Kennedy,[b] and Callum J. McHugh*[a]*

[a] School of Science and Sport, University of the West of Scotland, Paisley, PA1 2BE, UK.

[b] Department of Pure & Applied Chemistry, University of Strathclyde, Glasgow, G1 1XL, UK.

[c] School of Life and Medical Sciences, University of Hertfordshire, Hatfield, AL10 9AB, UK.

*Corresponding authors: callum.mchugh@uws.ac.uk, j.calvo-castro@herts.ac.uk

**ABSTRACT:** Rationalising the effects of molecular substitution in π-conjugated organic materials arising from well-defined intermolecular interactions, which can influence the formation of predefined packing motifs and control the emergence of π-π stacking represents a current challenge in supramolecular design. Significant effort is potentially required to manage the impact on solid state packing behaviour in materials that have been molecularly tuned to carry out specific photophysical and electrochemical functions. In this regard, fluorine substitution in π-conjugated systems has seen a recent surge of interest, primarily aimed towards

the development of materials with enhanced optical and optoelectronic behaviour. In light of this interest, in the following study, we report the synthesis and single crystal structures from a series of four novel and structurally related, symmetric, fluorinated N-benzyl substituted diketopyrrolopyrroles (DPPs). Two of the investigated series exhibit slipped cofacial π-π dimer pairs, which are consistent with those reported by us previously in halogenated DPPs. Significantly, this characteristic stacking motif of N-benzyl substituted DPPs can be carefully modified via the replacement of hydrogen atoms with trifluoromethyl and isosteric fluorine-hydrogen substituents. In the case of trifluoromethyl substitution, we identify a previously unobserved packing motif exhibiting a framework of well-defined channels propagating along the length of the crystallographic *c*-axis. In each of the reported systems all of the nearest neighbour dimer pairs have been identified and their intermolecular interaction energies computed by means of M06-2X density functional at 6-311G(d) level. Through a detailed theoretical analysis involving the determination of cropped dimer energetics, organic fluorine is shown to play an active role in the stabilisation of the crystal extracted dimer pairs through a number of additive and weak C-F---H, C-F---$\pi_F$ and C-F---π intermolecular contacts. Contrary to recent reports, we demonstrate that substitution of hydrogen by fluorine can also lead to dramatic changes in solid state packing behaviour as a consequence of these weak interactions. Given the importance of organic fluorine substitution in the construction of π-conjugated materials for optoelectronic materials we feel that this work should be of interest to the wider community involved in supramolecular design of organic conjugated systems, and in particular to those investigating organic fluorine as well as diketopyrrolopyrrole containing architectures.

## INTRODUCTION

Historically, diketopyrrolopyrroles (DPPs) have been widely utilised in industry as high performance pigments in view of their exceptional properties such as brightness as well as light and weather fastness.[1-5] More recently, DPP based technologies have emerged as promising charge transfer mediating materials in optoelectronic devices such as organic light emitting diodes, organic field effect transistors as well as in solar energy conversion technologies such as dye sensitised solar cells and organic photovoltaics.[6-17] We are currently engaged in the design of novel crystalline and thin film DPP platforms[18-20] with a view to developing an in-depth understanding of their crystallographic intermolecular interactions, aimed towards the rational design of sensing applications[18], where the signal transduction can be either optical or optoelectronic. In this regard, small structural changes have been observed to exert dramatic changes to intermonomer interactions and hence associated charge transfer properties,[19-22] which in N-benzyl substituted DPPs are related to characteristic slipped cofacial π-π stacking dimer pairs, closely aligned along their short molecular axes upon N-substitution.[19] Understanding the role of functional groups and substituent effects in these systems, which can facilitate or disrupt the formation of those desirable packing motifs, via well-defined interactions is crucially important in supramolecular design. There remains an identified need for studies, such as the one reported herein, where systematic substitutions are performed on a common core structure and the effects of manipulating the crystal lattice and intermolecular packing interactions are explored in-depth. In this work, we focus our interests on the role of organic fluorine in influencing the crystal structures and 1-dimensional π-π stacks in a series of N-benzyl substituted DPPs. In recent years, studies involving the interactions of fluorine substituents have seen a surge of interest, particularly in the fields of life sciences and solid state materials.[23] Fluorine is often used in substitutions of hydrogen atoms given their similar polarizabilities; however, this

isosteric substitution is associated to a significant change in occupied volume. Upon substitution, physical and chemical properties in these types of comparative systems are known to be significantly affected given the different electronegativities of the atoms involved.[23-25] As an example, the electron density of a perfluorinated ring is reversed compared to that of its non-fluorinated analogue. In crystalline environments, organic fluorine can participate in a series of intermolecular interactions such as C-F---H, C-F---F-C, C-F---$\pi_F$ and $\pi$-$\pi_F$.[23-28] Despite its large electronegativity however, organic fluorine rarely forms H-bonding intermolecular interactions and these are often restricted to specific cases when their formation involving much better acceptor atoms such as oxygen and nitrogen are sterically hindered.[24,25,29] Although normally weak, these interactions can however induce significant structural changes in the solid state.[23] Therefore, despite an increasing understanding of the role played by organic fluorine in influencing intermolecular interactions and packing behaviour, additional studies addressing the key role fluorine plays in crystal engineering are warranted. This is particularly appropriate in the development of DPP based materials, where reports of fluorine substitution are limited and have not involved an in-depth and systematic crystallographic analysis.[30-32]

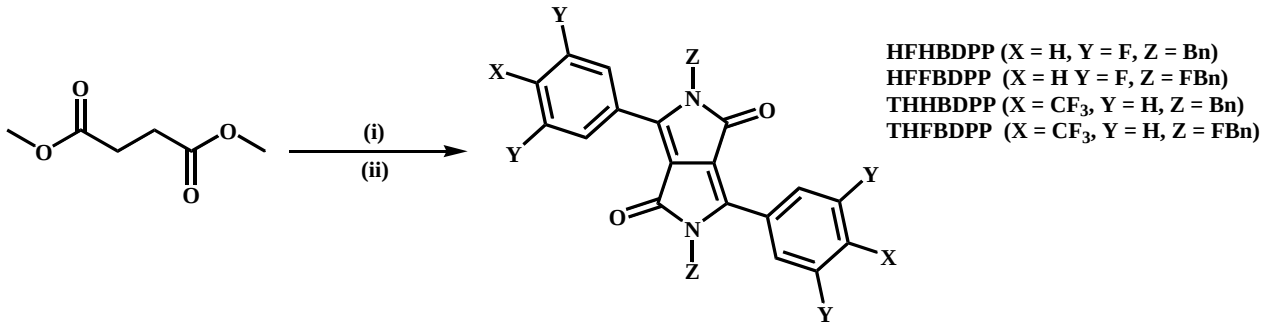


**Scheme 1**. DPP synthetic route. (i) PhCNXY, Na, t-amyl alcohol, reflux; (ii) BnBr or pentafluoro-BnBr, $K_2CO_3$, DMF, 120 °C;

To this end, we report the synthesis, determination and characterisation of a series of four symmetric, fluorinated N-benzyl substituted DPP single crystal structures (Scheme 1). The four structures, ***HFHBDPP***, ***HFFBDPP***, ***THHBDPP*** and ***THFBDPP*** were given names with a form of ***XYZDPP*** arising from their topology (see Figure 1) where **X** and **Y** denote the substitution of the para and meta positions of the phenyl rings attached to the central DPP core respectively. In turn, **Z** represents isosteric substitution of the phenylic hydrogen atoms for fluorine atoms within the benzyl groups.

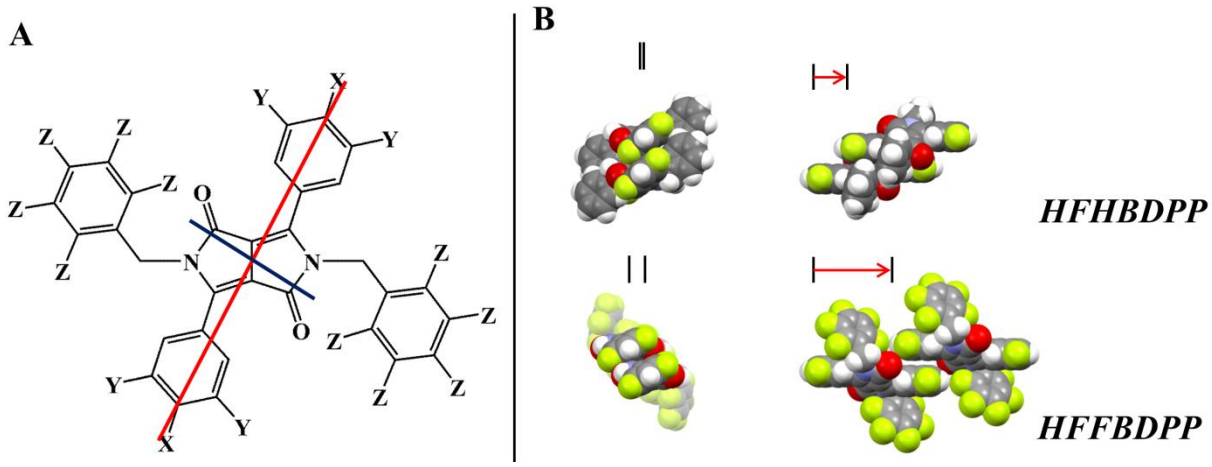


**Figure 1**. Illustration of long and short molecular axes of DPP based systems (left). Long and short molecular axis view of π-π dimer pairs of ***HFHBDPP*** (top) and ***HFFBDPP*** (bottom). Phenyl-DPP cores in short molecular axis view of ***HFFBDPP*** are highlighted for ease of visualisation.It is worthwhile to note that two of the structures reported herein; namely ***HFHBDPP*** and ***HFFBDPP*** exhibit 1-dimensional slipped cofacial π-π stacks consistent with those reported by us previously.[19] This type of packing behaviour is often thought to represent a key structural feature leading to the emergence of semiconductor bandwidths in organic crystalline materials.[19,21,22] The degree of long and short molecular axis slip is markedly different

in both structures, which we attribute to effects of DPP core phenyl versus benzyl fluorination. Thus, ***HFHBDPP*** exhibits a cofacial arrangement of monomers in the π-π stacks with a long molecular axis slip (Δx) of 3.72 Å and short molecular axis slip (Δy) of 0.35 Å. This arrangement of monomers is entirely consistent with the previously reported non-fluorinated equivalent (***HHHBDPP***) where Δx = 4.50 Å and Δy = 0.30 Å. In turn, additional fluorination of the benzyl substituents affords an extreme slipped arrangement of monomers in the π-π stacks with Δx and Δy equal to 9.12 Å and 2.31 Å respectively. In this case, the structure deviates from our previous halogenated series with an increase in the short molecular axis slip. It is therefore clearly apparent in this system, that direct fluorination of the core phenyl and benzyl ring systems can afford changes in crystal packing (and molecular conformation, vide infra) which may contribute to a significant impact in both the predicted magnitude and sign of charge carriers (vide infra). In contrast to direct fluorination, trifluoromethyl substitution on the para position of the phenyl rings attached to the central DPP core is manifest in considerable disruption to the characteristic slipped packing motif in both ***THHBDPP*** and ***THFBDPP***. The latter structure in particular, whereby the N-benzyl substituents were also fluorinated exhibits a highly unusual cofacial dimer pair arrangement where the monomers are offset with respect to their short molecular axis by ca. 46°. An orthogonal arrangement of the repeating units produced by the dimer pairs in this structure results in the formation of channels that perpetuate along the length of the crystallographic *c* axis (vide infra). From a search of the Cambridge Structural Database (CSD) this is the first reported DPP structure displaying this type of packing motif and as a result, is of particular interest and will be extensively discussed herein.

In summary, given the current interest in fluorine based π-conjugated materials in optical and optoelectronic applications and the key role played by crystal structure in defining the efficiency

and behaviour of solid state devices, we feel that this study should be of wide interest to those engaged in the engineering of novel organic charge transfer mediating materials as well as to those interested in developing an in-depth understanding of intermolecular interactions in π-conjugated systems, in particular involving organic fluorine.

## EXPERIMENTAL SECTION

**Reagents and instrumentation.** Unless otherwise specified, all starting materials and reagents were purchased from Fisher Scientific, Sigma-Aldrich or VWR and used as received without further purification. $^{1}$H NMR and $^{13}$C NMR spectra were determined using a Bruker AV3 400 MHz spectrometer (in $CDCl_3$) provided by the University of Strathclyde in Glasgow, UK. Elemental analyses were carried out using the service provided by the University of Strathclyde in Glasgow, UK. FTIR analyses were carried out on the neat samples by attenuated total reflectance using a Thermo Scientific Nicolet iS5 FTIR Spectrometer, with an iD5 ATR (Diamond) sampling accessory.

**Synthesis.** 3,6-bis(3,5-difluorophenyl)-2,5-dihydropyrrolo[3,4-*c*]pyrrole-1,4-dione (***HFDPP***). 3,5-difluorobenzonitrile was added to a solution of sodium t-amyloxide, prepared by dissolving sodium metal wire (0.91 g, 39.56 mmol) in anhydrous 2-methyl-2-butanol (30 mL), and the resulting mixture heated to reflux. Under vigorous stirring, dimethyl succinate (1.11 g, 7.60 mmol) dissolved in anhydrous 2-methyl-2-butanol (18.5 mL) was added over 1.5 h. After further stirring for 2 h at reflux temperature, the mixture was cooled to 60 °C and treated with methanol (15 mL) and hydrochloric acid (37 %, 10 mL). The precipitate was collected by filtration, washed with water, methanol and dichloromethane and then dried to give ***HFHDPP***

(1.55 g, 56.6 %) as a red powder. IR (ATR)/$cm^{-1}$: 3151 (NH), 3083 (ArH), 3048 (ArH), 3021 (ArH), 1651 (C=O), 1592 (NH), 1581 (C=C), 1136 (CF), 734 (ArH). Anal. Calcd. for $C_{18}H_8F_4N_2O_2$: C, 60.01; H, 2.24; N, 7.78. Found: C, 57.78; H, 1.94; N, 7.10. Melting Point: > 400 °C.

3,6-bis[4-(trifluoromethyl)phenyl]-2,5-dihydropyrrolo[3,4-c]pyrrole-1,4-dione **(*THDPP*)**. As per the method described for ***HFDPP*** using sodium metal wire (0.73 g, 31.74 mmol) in 2-methyl-2-butanol (25 mL), 4-(trifluoromethyl)benzonitrile (2.53 g, 14.78 mmol) and dimethyl succinate (0.92 g, 6.29 mmol) in 2-methyl-2-butanol (14.5 mL). The product ***THDPP*** (1.74 g, 65.2 %) was obtained as a red powder. IR (ATR)/$cm^{-1}$: 3142 (NH), 3082 (ArH), 3039 (ArH), 2984 (ArH), 1637 (C=O), 1600 (NH), 1586 (C=C), 1440 (C=C), 1315 (C-F), 679 (ArH). Anal. Calcd. for $C_{20}H_{10}F_6N_2O_2$: C, 56.61; H, 2.38; N, 6.60. Found: C, 53.37; H, 1.72; N, 6.18. Melting Point: > 400 °C.

2,5-dibenzyl-3,6-bis(3,5-difluorophenyl)pyrrolo[3,4-*c*]pyrrole-1,4-dione (***HFHBDPP***). A suspension of ***HFDPP*** (0.40 g, 1.11 mmol) and anhydrous $K_2CO_3$ (1.66 g, 12.01 mmol) in anhydrous DMF (20 mL) was heated at 120 °C under nitrogen atmosphere. At this temperature and under vigorous stirring a benzyl bromide (1.87 ml, 11.00 mmol) solution in DMF (10 ml) was added over 1 h. Stirring and heating at 120 °C were continued for 1 h and after cooling to room temperature salt was filtered and washed with DMF. After precipitation with methanol the crude product was purified by wet flash chromatography eluting with hexane-dichloromethane (7:3) to give ***HFHBDPP*** (0.11 g, 18.3 %) as a bright orange powder. $^1$H NMR ($CDCl_3$): 5.00 (4H, s, $CH_2$); 6.93-6.98 (2H, m, ArH), 7.18-7.20 (4H, m, ArH), 7.27-7.37 (10H, m ArH). $^{13}$C

NMR ($CDCl_3$): 45.69, 106.77, 107.01, 107.26, 110.41, 111.98, 112.06, 112.18, 112.26, 126.62, 127.81, 129.01, 130.12, 130.17, 130.32, 136.61, 146.99, 161.66, 161.80, 162.03, 164.15, 164.30. IR (ATR)/$cm^{-1}$: 3074 (ArH), 3029 (ArH), 2920 ($CH_2$), 1682 (C=O), 1582 (C=C), 1438 ($CH_2$), 1385 ($CH_2$), 1133 (CF), 737 (ArH). Anal. Calcd. for $C_{32}H_{20}F_4N_2O_2$: C, 71.11; H, 3.73; N, 5.18. Found: C, 71.39; H, 3.89; N, 5.13. TLC: $R_f$ (dichloromethane) 0.42, (ethyl acetate) 0.77. Melting Point: 222-224 °C

2,5-bis(pentafluorobenzyl)-3,6-bis(3,5-difluorophenyl)pyrrolo[3,4-*c*]pyrrole-1,4-dione (***HFFBDPP***). As per the method described for ***HFHBDPP*** from ***HFDPP*** (0.72 g, 2.00 mmol), anhydrous potassium carbonate (0.30 g, 2.17 mmol), anhydrous DMF (50 mL) and 2,3,4,5,6-pentafluorobenzyl bromide (0.58 g, 2.22 mmol) dissolved in anhydrous DMF (30 mL). Purification of the crude product by wet flash column chromatography eluting with hexane-dichloromethane (1:1) followed by precipitation with methanol gave ***HFFBDPP*** (0.045 g, 5.62 %) as a bright yellow powder. $^1$H NMR ($CDCl_3$): 5.05 (4H, s, $CH_2$), 6.98-7.03 (2H, m, ArH) 7.22-7.25 (4H, m, ArH). $^{13}$C NMR ($CDCl_3$): 34.42, 107.05, 107.29, 107.57, 109.19, 109.29, 110.44, 111.58, 111.85, 129.48, 129.57, 129.66, 136.27, 138.69, 139.86, 142.34, 143.83, 146.13, 146.31, 160.99, 161.74, 161.91, 164.24, 164.36. IR (ATR)/$cm^{-1}$: 3093 (ArH), 3057 (ArH), 2960 ($CH_2$), 2921 ($CH_2$), 1695 (C=O), 1589 (C=C), 1502 (C=C), 1436 ($CH_2$), 1386 ($CH_2$), 1125 (CF), 694 (ArH). Anal. Calcd. for $C_{32}H_{10}F_{14}N_2O_2$: C, 53.35; H, 1.40; N, 3.89. Found: C, 53.27; H, 0.98; N, 3.76. TLC: $R_f$ (dichloromethane) 0.50, (ethyl acetate) 0.75. Melting Point: 268-270 °C

2,5-dibenzyl-3,6-bis[4-(trifluoromethyl)phenyl]pyrrolo[3,4-*c*]pyrrole-1,4-dione (***THHBDPP***). As per the method described for ***HFHBDPP*** from ***THDPP*** (0.60 g, 1.41 mmol), anhydrous

potassium carbonate (2.17 g, 15.70 mmol), anhydrous DMF (25 mL) and benzyl bromide (2.43 g, 14.29 mmol). After precipitation with methanol, purification of the crude product by wet flash column chromatography eluting with hexane-dichloromethane (1:1) gave ***THHBDPP*** (0.21 g, 24.7% yield) as a bright yellow powder. $^{1}$H NMR ($CDCl_3$): 4.99 (4H, s, $CH_2$), 7.19-7.21 (4H, m, ArH), 7.27-7.36 (6H, m, ArH), 7.72 (4H, d, ArH), 7.88 (4H, d, ArH). $^{13}$C NMR ($CDCl_3$): 45.69, 110.57, 122.15, 124.85, 125.88, 126.60, 127.73, 128.98, 129.38, 130.94, 132.44, 132.77, 133.11, 133.42, 136.85, 147.97, 162.37. IR (ATR)/cm$^{-1}$: 3081 (ArCH), 3034 (ArCH), 2940 ($CH_2$), 1678 (C=O), 1609 (C=C), 1437 (C=C), 1409 ($CH_2$), 1377 ($CH_2$), 1321 (CF), 1106 (CF), 1069 (CF), 667 (ArCH). Anal. Calcd. for $C_{34}H_{22}F_6N_2O_2$: C, 67.55; H, 3.67; N, 4.63. Found: C, 67.10; H, 3.32; N, 4.59. TLC: $R_f$ (dichloromethane) 0.54, (ethyl acetate) 0.79. Melting Point: 262-264 °C

2,5-bis(pentafluorobenzyl)-3,6-bis[4-(trifluoromethyl)phenyl]pyrrolo[3,4-*c*]pyrrole-1,4-dione (***THFBDPP***). As per the method described for ***HFHBDPP*** from ***THDPP*** (0.85 g, 2.00 mmol), anhydrous potassium carbonate (0.30 g, 2.17 mmol), anhydrous DMF (50 mL) and 2,3,4,5,6-pentafluorobenzyl bromide (0.50 g, 1.92 mmol) dissolved in anhydrous DMF (30 mL). Purification of the crude product by wet flash column chromatography eluting with hexane-dichloromethane (3:2) and precipitation with methanol gave ***THFBDPP*** as a bright yellow powder (0.122 g, 16.24%). $^{1}$H NMR ($CDCl_3$): 5.04 (4H, s, $CH_2$), 7.80 (8H, m, ArH). $^{13}$C NMR ($CDCl_3$): 34.39, 109.25, 110.51, 119.27, 121.99, 124.69, 126.13, 128.92, 130.45, 132.74, 133.08, 133.42, 133.72, 136.11, 138.63, 139.82, 142.36, 143.83, 146.31, 147.14, 161.32. IR (ATR)/cm$^{-1}$: 2944 ($CH_2$), 1679 (C=O), 1609 (C=C), 1499 (C=C), 1418 ($CH_2$), 1376 ($CH_2$), 1328 (CF), 1127 (CF), 1114 (CF), 1066 (CF), 669 (ArH). Anal. Calcd. for $C_{34}H_{12}F_{16}N_2O_2$: C, 52.06; H, 1.54; N,

3.57. Found: C, 52.18; H, 1.05; N, 3.57. TLC: $R_f$ (dichloromethane) 0.63, (ethyl acetate) 0.83. Melting Point: 281-283 °C

**Preparation of Crystals for Single Crystal X-Ray Diffraction analysis.** All of the crystals were obtained from DCM/hexane (1:1) by slow evaporation of a cooled solution.

**Crystal structure determination.** All measurements were made with Oxford Diffraction instruments. Refinement was to convergence against $F^2$ and used all unique reflections. Programs used were from the SHELX suite.[33] Hydrogen atoms were placed in idealized positions and refined in riding modes. The $CF_3$ group of ***THFBDPP*** was modelled as disordered over two sites with occupancies refined to 0.595(4) and 0.405(4). These disordered groups required restraints and constraints to be applied to displacement parameters. Selected crystallographic and refinement parameters are given in Table 1. CCDC reference numbers 1449852-1449855 contain the supplementary crystallographic data for this paper. These data can be obtained free of charge from The Cambridge Crystallographic Data Centre via www.ccdc.cam.ac.uk/data_request/cif.

**Table 1**. Selected crystallographic data and refinement parameters for ***XYZBDPP*** compounds

| **Compound** | ***HFHBDPP*** | ***HFFBDPP*** | ***THHBDPP*** | ***THFBDPP*** |
|---|---|---|---|---|
| **Formula** | $C_{32}H_{20}F_4N_2O_2$ | $C_{32}H_{10}F_{14}N_2O_2$ | $C_{34}H_{22}F_6N_2O_2$ | $C_{34}H_{12}F_{16}N_2O_2$ |
| **$M_r$ (g mol$^{-1}$)** | 540.50 | 720.42 | 604.53 | 784.46 |
| **Crystal system** | monoclinic | monoclinic | monoclinic | tetragonal |
| **Space group** | $P2_1/c$ | $P2_1/c$ | $P2_1/c$ | P-4b2 |
| **Temperature (K)** | 123(2) | 123(2) | 123(2) | 123(2) |

| | | | | |
|---|---|---|---|---|
| ***a* (Å)** | 5.6106(3) | 9.1947(4) | 15.2024(18) | 18.5781(3) |
| ***b* (Å)** | 24.1920(15) | 9.8373(4) | 9.3312(11) | 18.5781(3) |
| ***c* (Å)** | 8.8718(5) | 15.3292(6) | 9.8704(11) | 9.2249(2) |
| **β (°)** | 91.853(5) | 91.889(4) | 104.458(11) | |
| ***V*/Å$^3$** | 1203.55(12) | 1385.79(10) | 1355.8(3) | 3183.94(10) |
| ***Z*** | 2 | 2 | 2 | 4 |
| **Wavelength (Å)** | 1.5418 | 1.5418 | 0.71073 | 1.5418 |
| **Measured reflections** | 4660 | 9895 | 6287 | 11986 |
| **Unique reflections** | 2340 | 2757 | 3165 | 3134 |
| **$R_{int}$** | 0.0274 | 0.0330 | 0.0453 | 0.0279 |
| **Observed rflns [*I* > 2σ(*I*)]** | 2013 | 2599 | 2405 | 2765 |
| **μ (mm$^{-1}$)** | 0.970 | 1.560 | 0.121 | 1.506 |
| **No. of parameters** | 181 | 226 | 199 | 257 |
| **2*θ*max (°)** | 146.52 | 146.36 | 53.98 | 146.22 |
| ***R* [on *F*, obs rflns only]** | 0.0449 | 0.0443 | 0.0571 | 0.0452 |
| ***wR* [on F$^2$, all data]** | 0.1292 | 0.1286 | 0.1441 | 0.1279 |
| **GoF** | 1.046 | 1.075 | 1.045 | 1.047 |
| **Largest diff. peak/hole/e Å$^{-3}$** | 0.281/–0.238 | 0.421/-0.251 | 0.508/-0.421 | 0.341/-0.196 |

**Computational details**. All molecular modelling studies were carried out using the density functionals indicated below as implemented in Spartan10 software.[34] Dimer interaction energies, $\Delta E_{CP}$, were all corrected for Basis Set Superposition Error (BSSE) using the counterpoise correction method of Boys and Bernardi.[35] Using a cut-off distance of van der Waals (VdW) radius + 0.3Å, all nearest neighbour dimer interaction energies of crystal extracted-dimer structures were calculated using the M06-2X density functional[36] and triple zeta 6-311G(d) basis set. This density functional has been shown to give good account of the dimer interaction energies of π-π interacting systems.[37,38] All results in the main text therefore refer to M06-2X/6-311G(d) calculations on crystal derived dimer species.

## RESULTS AND DISCUSSION

**Structural description**. It has previously been shown[19] that in the solid state the unsubstituted parent molecule ***HHHBDPP*** and its 4-halogenated derivatives ***XHHBDPP*** (X = Cl, Br, I and B = benzyl) form a structural series. All of these molecules are crystallographically centrosymmetric and have conformations with the rings of the benzyl substituents mutually *anti* with respect to the DPP plane. They all adopt structures bases on slipped cofacial π-π dimer pairs of molecules. Moreover, there is a systematic variation in these interactions with increasing size of X leading to increasing amounts of slip along the long molecular axis. This means that for X = H and Cl (β form) the closest π-π contacts are between the DPP units and the $C_6H_4X$ rings whilst for the more slipped X = Br and I the closest π-π contacts are between pairs of $C_6H_4X$ rings, see Figures 1a and 1b. In all four cases the individual π-π dimer pairs stack to give infinite 1-dimensional constructs in which the individual DPP rings are parallel to one another.

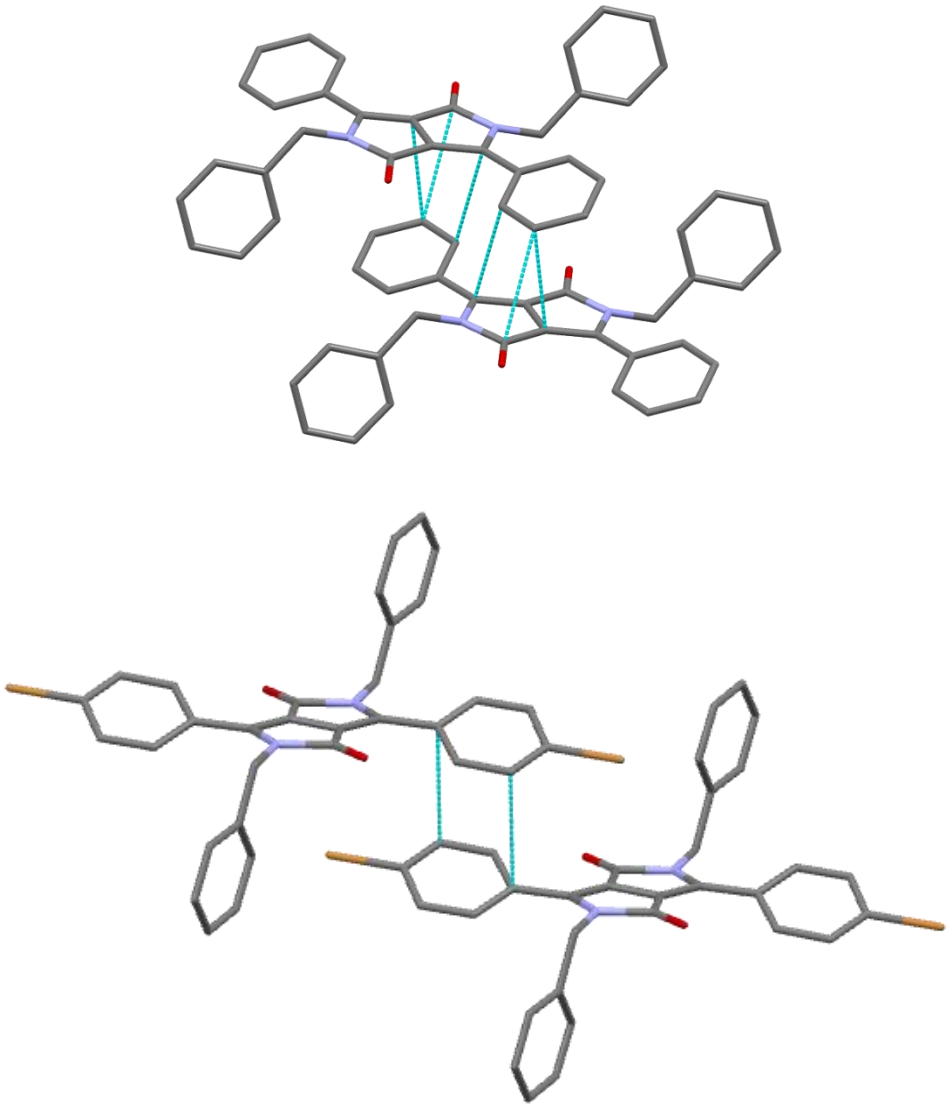

**Figure 2**. Dimeric contacts in (a) ***HHHBDPP*** top and (b) ***BrHHBDPP*** bottom. In both cases 1- dimensional stacks are formed form the individual cofacial π-π dimers, but the degree of slip differs such that in (a) the closest contacts are between the DPP and phenyl rings but in (b) the closest contacts are between pairs of $C_6H_4Br$ rings.[19]

The fluorinated species described here do not all conform to this structural type. ***HFHBDPP***, ***HFFBDPP*** and ***THHBDPP*** do have similar centrosymmetric molecular structures (Z' = 0.5) with *anti* conformations of the benzyl or $CH_2C_6F_5$ groups. However, ***THFBDPP*** adopts an

entirely different molecular conformation. Again Z' = 0.5 but here this is due to a two-fold rotation axis passing through the centre of the DPP group and perpendicular to the DPP plane. This gives a *syn* arrangement of the $CH_2C_6F_5$ substituents and this appears to sterically prevent one side of the DPP plane from forming close π-π contacts, see below.

Like the earlier reported ***XHHBDPP*** species, ***HFHBDPP*** and ***HFFBDPP*** do form intermolecular one dimensional polymers that are propagated by π-π contacts. Indeed ***HFHBDPP*** has a structure closely related to those of the ***XHHBDPP*** species. Like them, it forms a similar 1-dimensional stack with close contacts between the halogenated aryl ring and the DPP core. Here the stacks lie parallel to the crystallographic *a* axis. Further analysis does though show some differences in the details of how these stacks are formed. Rather than short C…C contacts as seen with ***XHHBDPP***, the shortest interactions with respect to van der Waals distances are now F…C contacts (3.052(2) Å) with the shortest C…C contacts being slightly longer than the sum of van de Waals distances (3.414(2) Å). To enable the short F…C contact, the plane of the fluorinated ring is much more twisted with respect to the plane of the rings of the DPP core (39.93(13) °) than in more planar ***XHHBDPP*** structures, compare Figure 3 with Figure 2a. The shortest C…C π-π contacts in ***HFHBDPP*** actually occur between its halogenated aromatic rings (shortest C…C 3.294(2) Å) rather than in the DPP/aryl stack. As can be seen in Figure 4, these contacts supported by C=O…H interactions, also give a polymeric 1-dimensional motif that cross links the earlier described stacks.

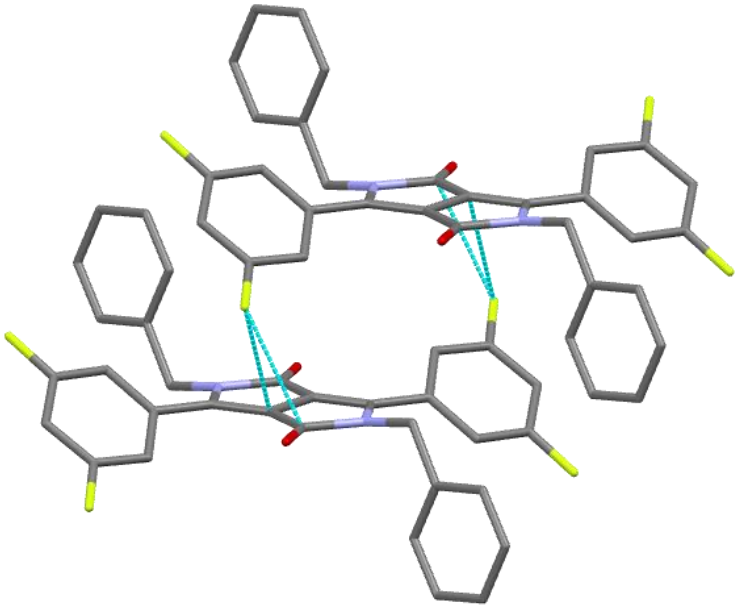

**Figure 3**. Dimeric interactions in ***HFHBDPP*** showing the close contacts between F and the **DPP** ring core. These interactions propagate to give a 1-dimensional stack parallel to the *a* axis.

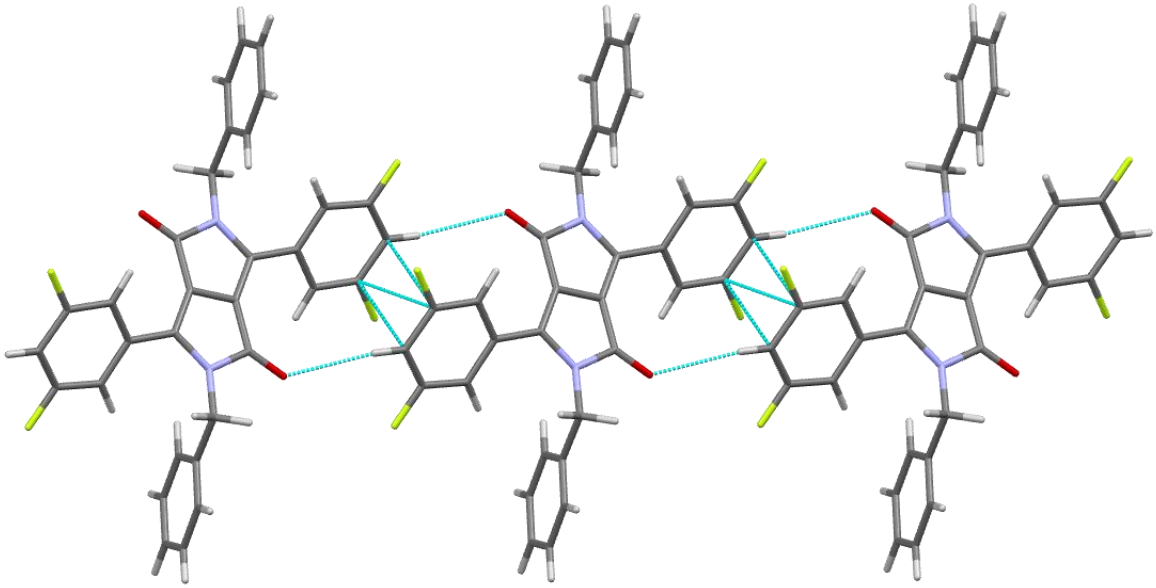

**Figure 4**. Interactions between pairs of $C_6H_3F_2$ rings give a second 1 dimensional construct based on π-π interactions in ***HFHBDPP***.

***HFFBDPP*** forms no π-π contacts shorter than the sum of van der Waals radii. Despite that, a stack of molecules somewhat similar to those seen for ***XHHBDPP*** (X = Br, I) and ***HFHBDPP*** is present. The dimer pair that forms the basis of these stacks is shown in Figure 5. Here neighbouring molecules have parallel $C_6H_3F_2$ rings but these are separated by distances longer than those usually considered significant (closest C…C contact 3.845(3) Å). This dimeric interaction may be supported by O…F and H…F interactions (3.017(2) and 2.61 Å respectively). Thus, this species may be described with the same slipped π-π stacked terminology and notation as used previously, but it should be noted that it presents an extreme form of this geometry. With respect to the sum of van der Waals radii, the shortest intermolecular distances in ***HFFBDPP*** are F…F and F…C contacts (closest contacts F…C 2.791(2) Å, F…F 2.8282(16) Å). Although the DPP core is involved here, the edge-to-face geometry of the contacts (see Figure 6) means that these are not cofacial π-π stacks.

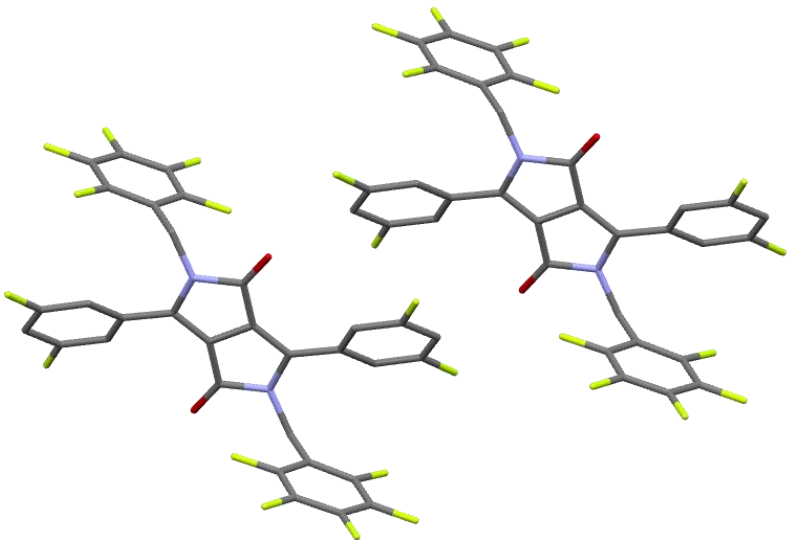

**Figure 5**. The π-π dimer that forms the basis of the 1 dimensional stack that propagates along the *b* direction and which is used to describe the structure and properties of ***HFFBDPP***. Compare this to Figure 2b.

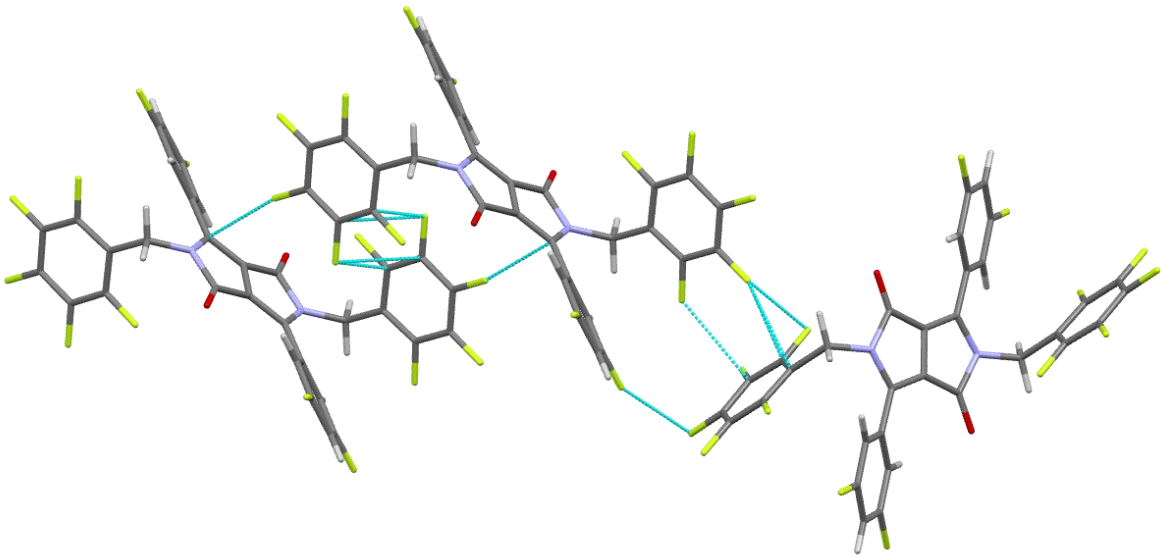

**Figure 6**. Part of the structure of ***HFFBDPP*** showing the F…F and F…C contacts that are the shortest contacts in this structure with respect to van der Waals distances.

The packing structures of the two $CF_3$ containing species cannot be described using the same stack of cofacial π-π dimer description employed for the previously discussed structures. Unlike any of the previously described species, ***THHBDPP*** forms π-π contacts not through interactions between its **DPP** and/or halogenated rings but instead through interactions of these groups with the ring of the benzyl group, see Figure 7. (Closest face to face benzyl to DPP contact is C…C 3.329(3) Å; benzyl to $C_6H_4CF_3$ contact is in edge to face mode through a C-H group of the $C_6H_4CF_3$ ring). Supported by C=O…H interactions this does form a 1-dimensional

intermolecular polymer, but it is very different in its construction from the slipped cofacial π-π stacks of ***XHHBDPP*** and ***HFHBDPP***.

For ***THFBDPP***, with the unusual *syn* geometry of its $CH_2C_6F_5$ groups, close face to face π-π contacts between adjacent **DPP** moieties do occur (shortest contact distances C…C 3.405(4) Å and N…C 3.208(3) Å) and give the dimeric units shown in Figure 8. However, due to the *syn* conformation of the molecules these do not stack to give polymeric features. Neighbouring dimers interact through F…C and F…F short contacts to give the packing structure shown in Figure 10 (note that this leaves void regions in the structure). These channels run parallel to the crystallographic *c* axis with a width (F…F) of approximately 6 Å.

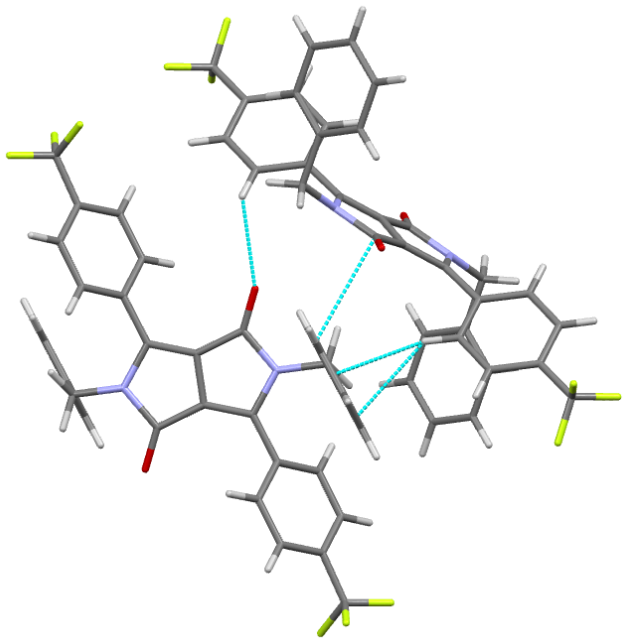

**Figure 7**. In the structure of ***THHBDPP*** the π-π contacts are based around interactions with the benzyl groups. This is in contrast to all the other structures described here and in reference 19.

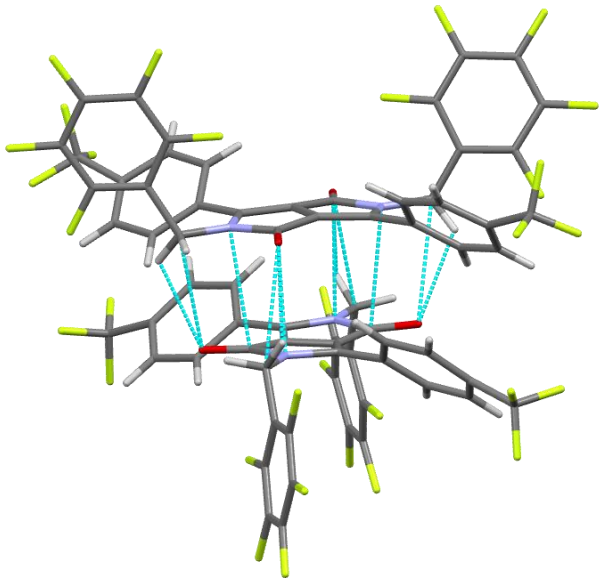

**Figure 8**. Face to face, **DPP** to **DPP** dimer formed by ***THFBDPP***. Note the unusual *syn* conformation of the molecules.

**Intermolecular interaction energies, $\Delta E_{CP}$.** Organic fluorine has been extensively reported to exhibit different types of intermolecular interactions such as C-F---H, C-F---F-C, C-F---$\pi_F$ and $\pi$-$\pi_F$. Although normally weak, these interactions can induce significant structural changes in crystalline environments[23] and as a consequence can play an active role in determining the solid state properties of organic optoelectronic materials. To further investigate the role of fluorine substitution in controlling and modifying the crystal structure and associated nearest neighbouring intermolecular interactions of the fluorinated N-benzyl substituted DPP materials reported herein, we computed $\Delta E_{CP}$ for their extracted crystalline dimer pairs following the method previously described for the ***XHHBDPP*** series.[19,20] All of the nearest neighbour dimer pairs within a cut-off distance of that of van der Waals radius + 0.3 Å were identified from the single crystal structures (SI1) of ***THHBDPP*** (10 neighbours), ***THFBDPP*** (8 neighbours), ***HFHBDPP*** (10 neighbours) and ***HFFBDPP*** (12 neighbours) and their intermolecular

interactions, $\Delta E_{CP}$ computed. In characterisation of the extracted dimer pairs , it is worthwhile to re-emphasis that in this case the DPP-based systems bearing trifluoromethyl substituents do not exhibit the distinctive slipped cofacial π-π dimer pairs observed previously with N-benzyl substituted DPPs.[18,19]

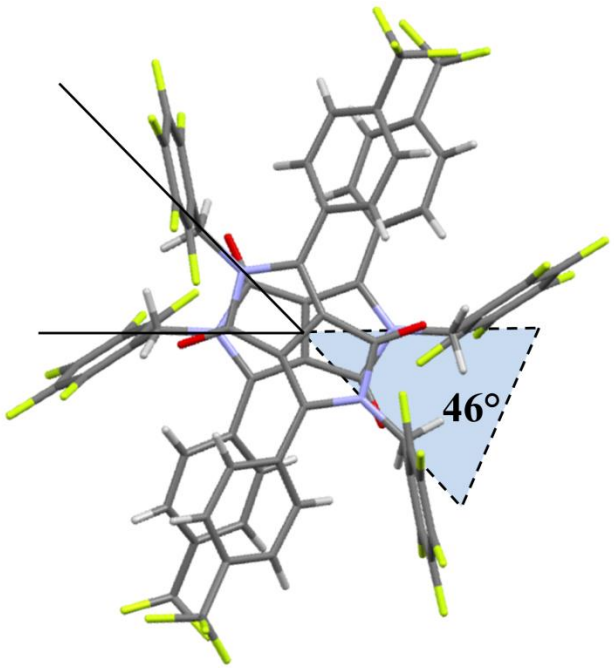


**Figure 9**. Dimer pair (II) of ***THFBDPP*** showing the 46° offset of their short molecular axes with respect to the centre of symmetry of the monomers.

Accordingly, the dimer pair (II) of ***THFBDPP*** was observed to exhibit a novel cofacial π-π stacking assembly (see Figures 9 and 10), with an intermonomer distance along the *z* axis of 3.36 Å. The crystallographic packing motif of ***THFBDPP***, does not exhibit the typical slipped cofacial stacking arrangement observed for other N-benzyl substituted diketopyrrolopyrroles.[19] In this case, the structure displays an alternating series of the cofacial π-π dimer pairs that are orthogonal to one another and which extend along the *a* and *b* crystallographic axes. This

crystallographic framework leads to the emergence of channels along the length of the crystallographic *c* axis. A section of these channels is illustrated in Figure 10, where the structure is observed to crudely adopt the form of an irregular octagon (with two different side lengths of ca 2.86 and 2.70 Å, inner angles of ca 40 and 50° and outer angles of ca 130 and 140°, unlike those of 45° and 135° respectively for a regular octagon) with a measured cross-sectional surface area of *ca* 40.50 $Å^2$. In this system, the short molecular axes of the monomers in the dimer pair are offset by 46° with respect to one another, as illustrated in Figure 9. Favourable attractive intermolecular interactions, as extracted from the large computed $\Delta E_{CP}$ of -127.55 kJ $mol^{-1}$ were observed, which greatly exceed those computed for the analogous, non-fluorinated N-benzyl substituted DPP systems ($\Delta E_{CP}$ = -70.20 and -69.90 kJ $mol^{-1}$ for ***HHHBDPP*** and ***ClHHBDPPβ*** respectively[19]). Thus, we propose significantly greater dimer thermal integrity should be anticipated for the dimer pair of ***THFBDPP***, along with the potential for unique optical, electronic and adsorption behaviour.

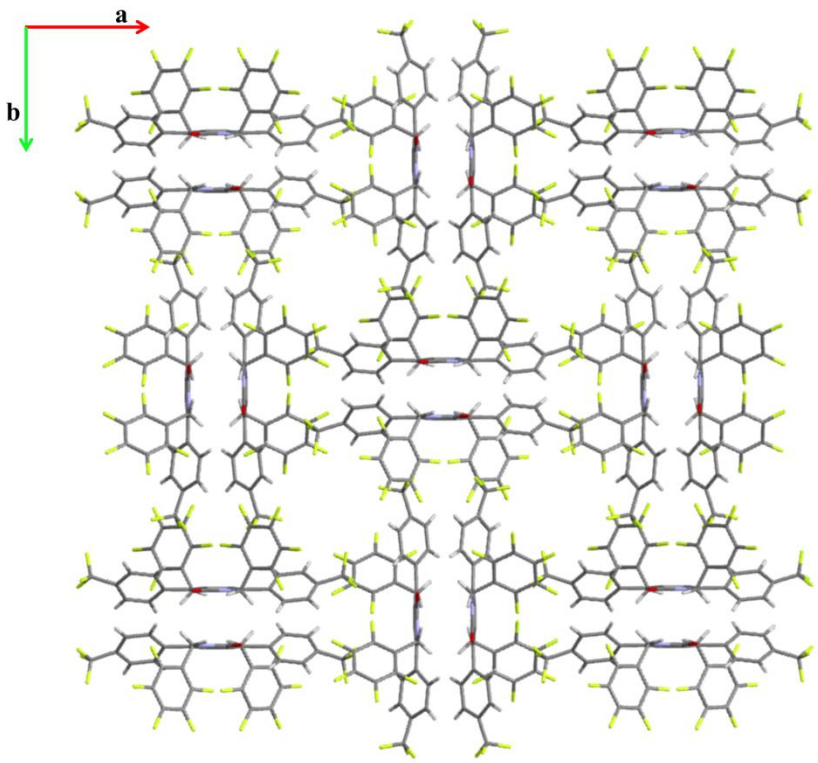


**Figure 10**. Capped stick illustration of the packing motif of ***THFBDPP*** as viewed along the crystallographic *c* axis.

The reported DPP systems bearing direct DPP core phenyl and benzyl fluorination, ***HFHBDPP*** and ***HFFBDPP***, exhibit characteristic[18,19] π-π stacking dimer pairs (see Figure 1) which propagate along their *a* and *b* crystallographic axes respectively. These π-π dimer pairs display intermonomeric displacements associated with Δx, Δy and Δz of 3.72, 0.35, 3.90 and 9.12, 2.31 and 3.59 Å for ***HFHBDPP*** and ***HFFBDPP*** respectively. The role of N-benzyl substitution in precluding any significant intermonomeric displacement along the short molecular axis in ***HFHBDPP*** is notable in a structure which also exhibits a small displacement along the long molecular axis. This is in close agreement with the global minimum (ca 3.50 Å) of our previously reported model systems for non-substituted DPP analogues,[19] and supports our assertion that N-benzyl substitution in DPP-based systems is associated to the preclusion of

significant displacements along the short molecular axis in these crystal structures, thereby favouring a slipped π-π stacking configuration and maximising potential wavefunction overlap.[18,19] This is in distinct contrast to the substantial short molecular axes shifts and herringbone packing arrangements exhibited by DPP pigments,[39-41] non-substituted acenes and thiophenes.[21,42-44] For the closely aligned π-π dimer pair of ***HFHBDPP*** (Δx = 3.72 Å) an intermolecular interaction energy of -71.02 kJ $mol^{-1}$ was computed, which is comparable to analogous N-benzyl diketopyrrolopyrroles (vide supra) and represents an almost two-fold increase in energy compared to the cofacial π-π dimer pair of rubrene, ($\Delta E_{CP}$ = -35.60 kJ $mol^{-1}$ computed using the same density functional and basis set) which is widely employed as a charge transfer mediating material.[45-47] This clearly indicates for ***HFHBDPP***, a great thermal integrity of the slipped cofacial π-π stacking dimer arrangement compared with rubrene. Large intermolecular interactions and associated thermal integrities play a crucial role in precluding small intermonomer displacements, which given the computed sensitivity of charge transfer integrals to small intermonomer shifts[19,21,22,48] represent a very desirable property in organic charge transfer mediating materials. Closer inspection of the structure from the non-fluorinated ***HHHBDPP*** equivalent reported previously,[19] reveals a number of subtle differences in intermolecular interactions that emerge as a consequence of DPP core phenyl fluorination. Both ***HHHBDPP*** and ***HFHBDPP*** display slipped π-π structures with comparable long and short molecular axes displacements (Δx = 4.50 Å and Δy = 0.30 Å for ***HHHBDPP*** and Δx = 3.72 Å and Δy = 0.35 Å for ***HFHBDPP***). As a result, both of the structures display very similar π-π stacking intermolecular interaction energies (-70.20 kJ $mol^{-1}$ and -71.02 kJ $mol^{-1}$ for ***HHHBDPP*** and ***HFHBDPP*** respectively). However, it is notable that the melting points of both single crystals are markedly different (278 °C and 222-224 °C for ***HHHBDPP*** and ***HFHBDPP***

respectively), which is crudely reflected in their total intermolecular interaction energies ($\Delta E_{CP}$ = -294 kJmol$^{-1}$ and -247 kJmol$^{-1}$ for ***HHHBDPP*** and ***HFHBDPP*** respectively). Differences in the overall interaction energies are consistent with the number of monomer nearest neighbours in each system with the 12 neighbours observed in the structure of ***HHHBDPP*** being reduced to only 10 in ***HFHBDPP***. Thus, despite a similarity in π-π stacking energies, it is apparent that fluorination of the DPP core phenyl rings in ***HFHBDPP*** has a negative impact on the overall crystal thermal stability compared to the non-fluorinated equivalent ***HHHBDPP***.

For ***HFFBDPP***, the lower computed intermolecular interaction energy (-22.46 kJ mol$^{-1}$) for the π-π stacking dimer pair can be readily understood on the basis of the associated intermonomer displacements (9.12, 2.31 and 3.59 Å for Δx, Δy and Δz respectively) upon fluorination of the benzyl groups. Whereas similar shifts along the long molecular axis have been previously observed for N-benzyl substituted DPPs,[19] the positive effect of the benzyl groups in precluding significant displacements along the long molecular axis and hence enhancing spatial intermonomer overlap was diminished upon isosteric substitution of the phenylic hydrogen atoms of the benzyl substituents. In light of this effect and considering the impact of $CF_3$ substitution observed in the structures of ***THHBDPP*** and ***THFBDPP*** we dedicate the remainder of the paper to the computation and analysis of the intermolecular interactions, $\Delta E_{CP}$ for all the nearest neighbours of the systems reported in an effort to broaden our understanding of fluorine-led interactions and their role in defining crystal packing motifs in N-benzyl substituted DPPs.

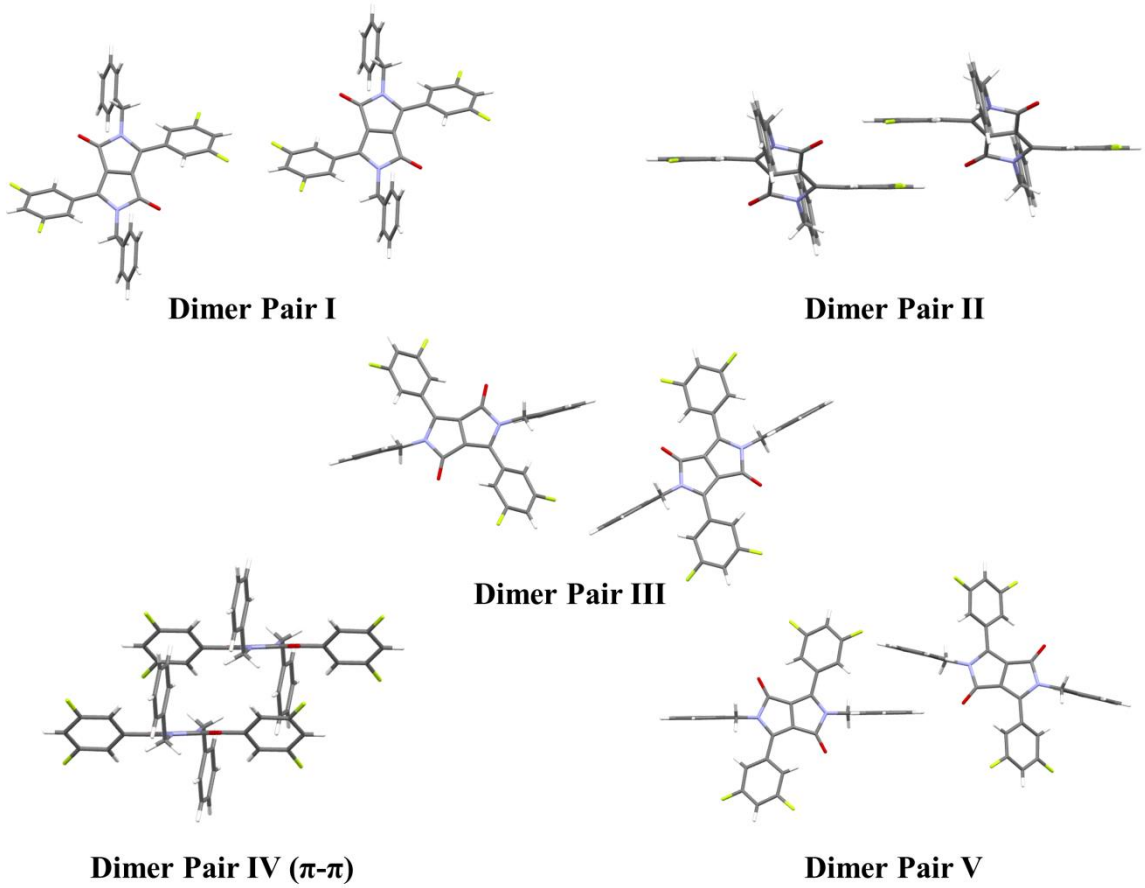


**Figure 11**. Capped stick illustration of the different nearest neighbour dimers of ***HFHBDPP***.

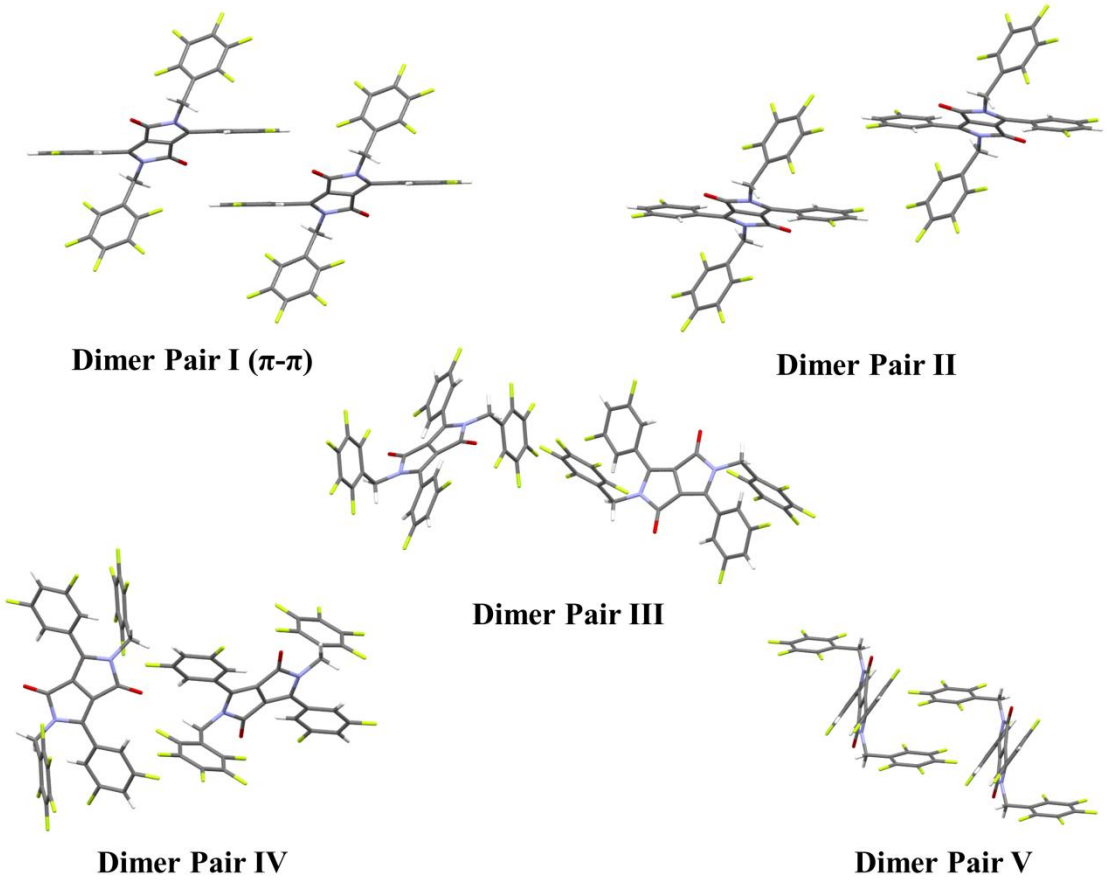


**Figure 12**. Capped stick illustration of the different nearest neighbour dimers of ***HFFBDPP***.

Figures 11 and 12 illustrate all of the identified nearest neighbour dimer pairs for ***HFHBDPP*** and ***HFFBDPP*** respectively from which intermolecular interactions were computed. The individual and simultaneous roles of benzyl/Zbenzyl (B) and Y substitution were investigated through a series of systematically cropped dimer pairs, consistent with our previously reported method.[19,20] In short, the benzyl groups (either fluorinated or non-fluorinated) and meta-fluoro substituents on the DPP core phenyl rings were cropped and substituted with hydrogen atoms; individually and then simultaneously, resulting in **YDPP**, **BDPP** and **DPP** structures respectively with ***YBDPP*** representing the uncropped dimer pairs. Tables 2 and 3 summarise the computed intermolecular interactions for the cropped and uncropped (structurally modified and non-

structurally modified) dimer pairs for the nearest neighbour dimer pairs of ***HFHBDPP*** and ***HFFBDPPP*** respectively.

**Table 2**. Counterpoise corrected intermolecular interactions energies, $\Delta E_{CP}$ for structurally modified and non-structurally modified dimer pairs of all the nearest neighbours of ***HFHBDPP***. M06-2X/6-311G(d)

| **Dimer pair** | **$\Delta E_{CP}$ / KJ mol$^{-1}$** | | | |
|---|---|---|---|---|
| | ***YBDPP*** | **YDPP** | **BDPP** | **DPP** |
| **I** | -5.36 | -6.77 | -0.84 | -0.51 |
| **II** | -25.77 | -27.94 | -27.91 | -28.68 |
| **III** | -1.56 | 0.05 | -1.35 | 0.38 |
| **IV (π-π)** | -71.02 | -30.96 | -76.17 | -36.37 |
| **V** | -19.75 | -0.36 | -17.90 | 0.22 |

**Table 3**. Counterpoise corrected intermolecular interactions energies, $\Delta E_{CP}$ for structurally modified and non-structurally modified dimer pairs of all the nearest neighbours of ***HFFBDPP***. M06-2X/6-311G(d)

| **Dimer pair** | **$\Delta E_{CP}$ / KJ mol$^{-1}$** | | | |
|---|---|---|---|---|
| | ***YBDPP*** | **YDPP** | **BDPP** | **DPP** |
| **I (π-π)** | -22.46 | -16.75 | -26.87 | -22.44 |
| **II** | -2.75 | -0.74 | -4.12 | -1.01 |
| **III** | -10.58 | 0.52 | -9.11 | 0.76 |
| **IV** | -28.51 | -13.92 | -17.43 | -9.59 |
| **V** | -28.15 | 0.73 | -25.25 | -0.25 |

We initially focus our discussion on the role of substituents on the π-π dimer pairs of ***HFHBDPP*** and ***HFFBDPP*** by means of their computed $\Delta E_{CPs}$. Notably, as opposed to other structurally related DPPs[19] and the structure of ***HFHBDPP*** reported herein, the π-π dimer pair of ***HFFBDPP*** does not exhibit the strongest interaction from all the nearest neighbour dimer pairs, which is related to the greater intermonomer displacements along the long and short molecular axes in this structure. Greater benzyl induced stabilisation in the π-π dimer pair of ***HFHBDPP*** ($\Delta E_{CP}$ = -71.02 and -30.96 kJ mol$^{-1}$ for associated ***YBDPP*** and **YDPP** dimer pairs) was observed

compared to the ***HFFBDPP*** analogue ($\Delta E_{CP}$ = -22.46 and -16.75 kJ mol$^{-1}$ for associated ***YBDPP*** and **YDPP** dimer pairs). This can be readily explained by comparing the different intermonomer displacements exhibited in each of the dimer pairs. The large benzyl induced stabilisation observed in ***HFHBDPP*** arises from the following contributions: slipped-cofacial[49-51] between the phenyl rings within the benzyl groups, slipped-cofacial between the phenyl rings attached to the DPP central core, a T-shape[52-64] attractive interaction between the benzylic phenyl rings and the phenyl rings linked to the DPP core and an electrostatic interaction between the electropositive methylene hydrogen atoms of one monomer and the electronegative carbonyl oxygens of the second monomer in the dimer pair, separated by a distance of 3.11 Å. In turn, π-π dimer pairs of ***HFFBDPP*** are primarily stabilised via cofacial intermolecular interactions of the phenyl rings attached to the DPP core, situated 3.82 Å apart, with limited benzyl stabilisation entirely attributed to the close contact (2.61 Å) of the para-phenylic hydrogen atom within the phenyl rings attached to the central core of one monomer and the ortho fluorine atom on the benzylic phenyl ring of the other monomer. In relation to any additional fluorine induced stabilisation[23-25,27,28,65-67] of these pairs, a close intermolecular contact between an electronegative fluorine atom and an electropositive phenylic hydrogen atom within the benzyl groups, separated by a distance of 2.72 Å was identified in the π-π dimer pair of ***HFHBDPP***. Surprisingly, removal of the fluorine atoms on progression from ***YBDPP*** to **BDPP** ($\Delta E_{CP}$ = -71.02 and -76.17 kJ mol$^{-1}$ respectively) and from **YDPP** to **DPP** ($\Delta E_{CP}$ = -30.96 and -36.37 kJ mol$^{-1}$ respectively) was associated with the emergence of larger computed stabilisation energies. This is consistent with a negligible fluorine induced stabilisation of this dimer pair despite the close contact, and more importantly with the newly formed attractive intermolecular interactions between electronegative carbonyl oxygen and substituted electropositive phenylic hydrogen

atoms separated by 3.11 Å. An analogous situation ($\Delta E_{CP}$ = -16.75 and -22.44 kJ mol$^{-1}$ for **YDPP** and **DPP** dimer pairs respectively) was identified for the π-π dimer pair of ***HFFBDPP*** upon isosteric substitution of the fluorine atoms for hydrogen atoms, with a stabilising H-bonding interaction being formed where the atoms were measured to be 3.02 Å apart.

For the remaining dimer pairs of ***HFHBDPP***, we identified an additional dimer pair (II), which is stabilised by a sole phenyl-phenyl slipped-cofacial intermolecular interaction ($\Delta z$ = 3.24 Å) and which exhibits a small benzyl/fluorine induced stabilisation as extracted from the computed $\Delta E_{CP}$ for the associated structurally modified dimer pairs (see Table 2 for details). In turn, systematic substitution plays a crucial role in the dimer pairs I and V of ***HFHBDPP*** (see Figure 11). The effect of fluorine induced stabilisation in dimer pair I can be determined via comparison of ***YBDPP*** and **BDPP** ($\Delta E_{CP}$ = -5.36 and -0.84 kJ mol$^{-1}$ respectively) as well as **YDPP** and **DPP** ($\Delta E_{CP}$ = -6.77 and -0.51 kJ mol$^{-1}$ respectively) associated dimer pairs, furthermore indicating negligible benzyl induced stabilisation. We attribute the fluorine induced stabilisation of this dimer to the close contact (2.62 Å) between the fluorine atoms of one monomer and para-phenylic hydrogen atoms of the other monomer in the pair. Dimer pair V was computed to be primarily stabilised via benzyl substitution. Stabilisation arises from two different contributions: slipped-cofacial interaction between the phenyl rings within the benzyl groups as well as an intermolecular H-bonding interaction between the electropositive methylene hydrogens and the electronegative carbonyl oxygens separated by a distance of 2.76 Å.

Dimer pairs III, IV and V of ***HFFBDPP*** were observed to exhibit clear substituent induced stabilisation, with dimer pairs III and V predominantly stabilised via the benzyl substituents, as inferred from the computed $\Delta E_{CP}$ for ***YBDPP*** and **YDPP** ($\Delta E_{CP}$ = -10.58 and 0.52 kJ mol$^{-1}$ for

dimer pair III and -28.15 and 0.73 kJ $mol^{-1}$ for V respectively) as well as **BDPP** and **DPP** ($\Delta E_{CP}$ = -9.11 and 0.76 kJ $mol^{-1}$ for dimer pair III and -25.25 and -0.25 kJ $mol^{-1}$ for dimer pair V respectively). In both cases, we attribute stabilisation to the interaction between the electronegative meta-fluorine atom within the benzylic phenyl rings and the electropositive methylene (dimer pair III) and ortho phenylic (dimer pair V) hydrogen atoms, distanced by 2.69 and 2.73 Å respectively. The greater benzyl stabilisation computed for dimer pair V is attributed to an intermolecular slipped cofacial interaction between the benzylic phenyl rings. For dimer pair IV, destabilisation of the system by 14.59 and 11.08 kJ $mol^{-1}$ was computed upon progression from ***YBDPP*** to **YDPP** and **BDPP** respectively. The computed destabilisation upon removal of the benzyl groups and fluorine atoms within the phenyl rings attached to the DPP core is consistent with the attractive intermolecular H-bonding interaction between the electronegative carbonyl oxygen and the electropositive methylene and ortho phenylic hydrogen atoms separated by a distance of 2.71 and 2.50 Å respectively. Furthermore, dimer pair IV is stabilised via intermolecular attractive interactions between the electropositive methylene hydrogen of one monomer and a meta-phenylic fluorine atom of the other monomer at 2.75 Å as well as by an interaction between the ortho-phenylic hydrogen and ortho-phenylic fluorine separated by a distance of 2.75 Å.

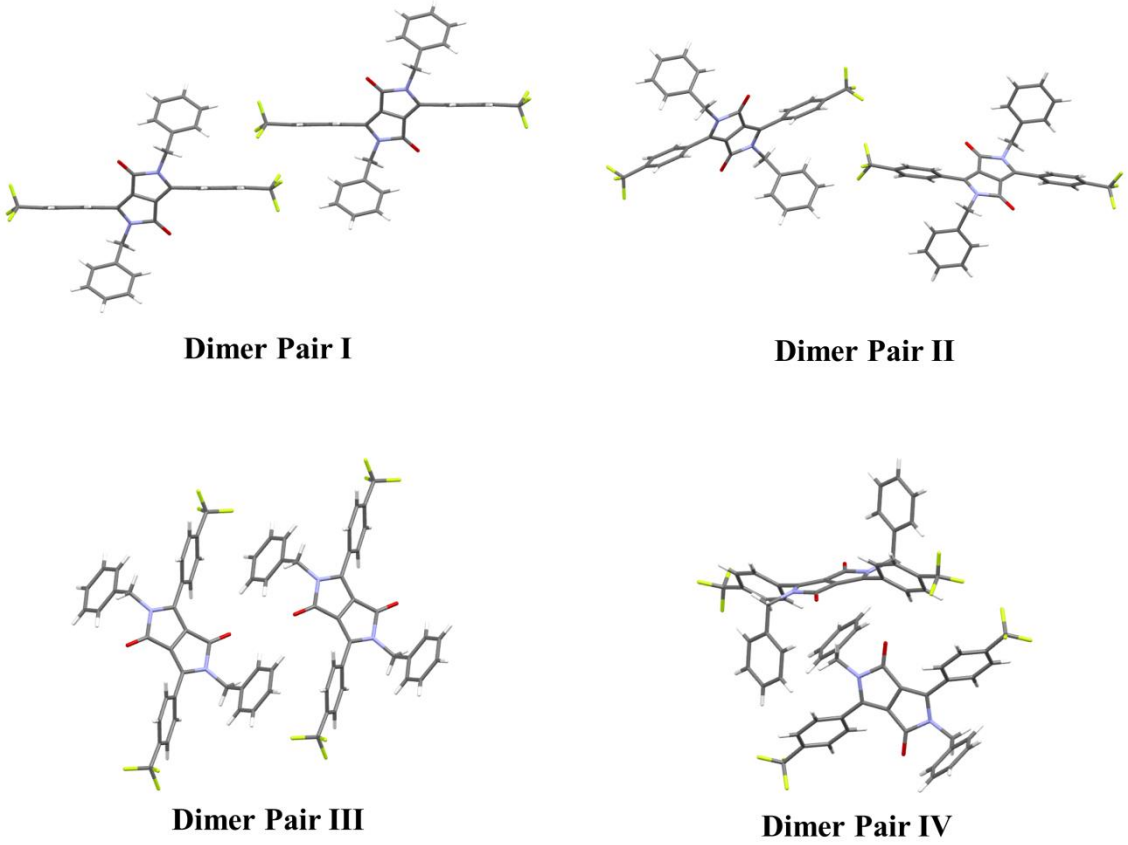


**Figure 13**. Capped stick illustration of the different nearest neighbour dimers of ***THHBDPP***.

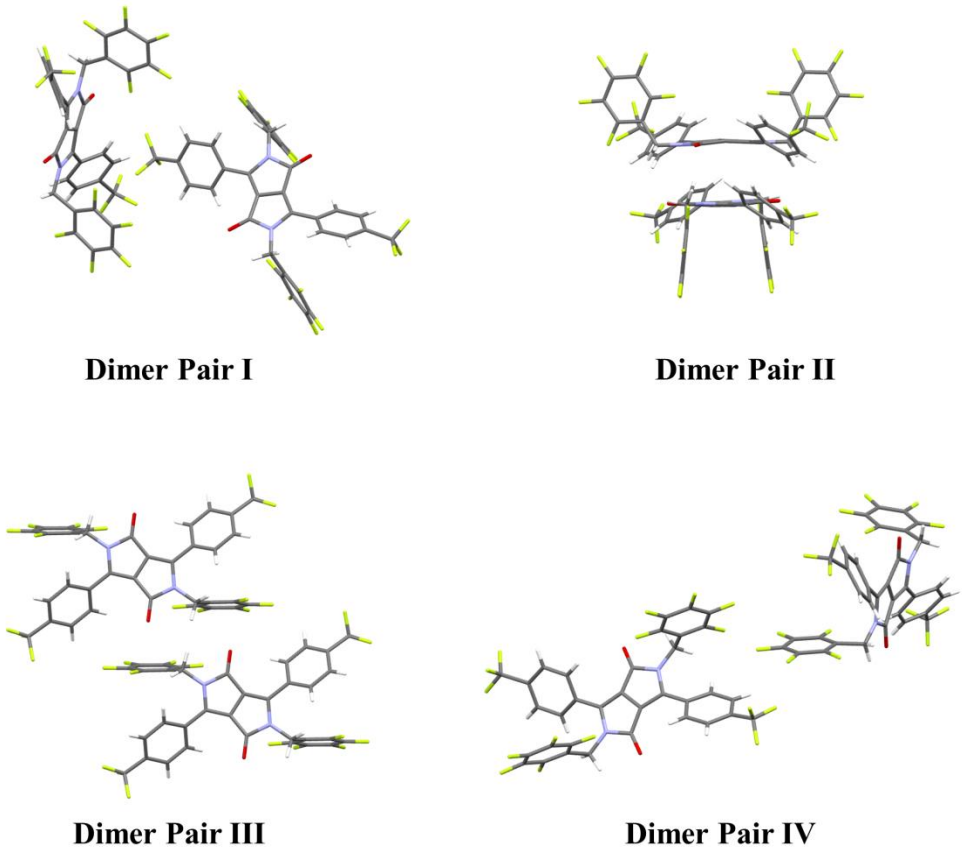


**Figure 14**. Capped stick illustration of the different nearest neighbour dimers of ***THFBDPP***.

All of the identified nearest neighbour dimer pairs for ***THHBDPP*** and ***THFBDPP*** are illustrated in Figures 13 and 14 respectively. Analogously to ***HFHBDPP*** and ***HFFBDPP***, the $\Delta E_{CP}$ were computed for all of the nearest neighbour dimer pairs within a distance equal to the Van der Waals radii + 0.30 Å. Stabilisation effects of the different substituents was examined in depth by means of a series of systematically cropped dimer pairs where the benzyl groups and the trifluoromethyl substituent were cropped and substituted with hydrogen atoms individually and then simultaneously, generating **XDPP**, **BDPP** and **DPP** respectively. Tables 4 and 5 summarise these computed intermolecular interactions for ***THHBDPP*** and ***THFBDPP*** respectively.

**Table 4**. Counterpoise corrected intermolecular interactions energies, $\Delta E_{CP}$ for structurally modified and non-structurally modified dimer pairs of the nearest neighbours of ***THHBDPP***. M06-2X/6-311G(d)

| **Dimer pair** | **$\Delta E_{CP}$ / KJ mol$^{-1}$** | | | |
|---|---|---|---|---|
| | ***XBDPP*** | **XDPP** | **BDPP** | **DPP** |
| **I** | -15.22 | -8.52 | -0.26 | -1.43 |
| **II** | -2.09 | -2.58 | -0.44 | -0.96 |
| **III** | -29.17 | -0.41 | -24.54 | 0.60 |
| **IV** | -45.47 | -12.63 | -39.31 | -8.92 |

**Table 5**. Counterpoise corrected intermolecular interactions energies, $\Delta E_{CP}$ for structurally modified and non-structurally modified dimer pairs of the nearest neighbours of ***THFBDPP***. M06-2X/6-311G(d)

| **Dimer pair** | **$\Delta E_{CP}$ / KJ mol$^{-1}$** | | | |
|---|---|---|---|---|
| | ***XBDPP*** | **XDPP** | **BDPP** | **DPP** |
| **I** | -12.68 | -6.60 | -3.92 | -0.88 |
| **II** | -127.55 | -104.47 | -124.61 | -97.32 |
| **III** | -38.55 | -12.67 | -40.02 | -11.59 |

| | | | | |
|---|---|---|---|---|
| **IV** | -9.03 | -0.26 | -3.68 | -0.02 |

From the computed $\Delta E_{CP}$ for the various dimer pairs of ***THHBDPP***, it was observed that dimer pairs I and II are primarily stabilised via attractive intermolecular interactions between electronegative fluorine atoms and electropositive ortho- and meta-phenylic hydrogens within the benzyl ring respectively, with associated distances of 2.86 and 2.68 Å for pairs I and II respectively. The much greater stability computed for dimer pair I upon removal of the trifluoromethyl group (14.96 and 1.65 kJ $mol^{-1}$ on progression from ***XBDPP*** to **BDPP** for dimer pairs I and II respectively) is attributed to an additional short contact between a fluorine atom and meta-phenylic hydrogen. In turn, dimer pair III is characterised by a greater destabilisation upon removal of the benzyl groups. This can be rationalised through comparison of the computed destabilisation energies on progression from ***XBDPP*** to **XDPP** and from **BDPP** to **DPP** (28.76 and 25.14 kJ $mol^{-1}$ respectively), which we attribute to a close (2.81 Å) attractive H-bonding interaction between the electronegative carbonyl oxygen and the electropositive meta-phenylic hydrogen atom of the benzyl groups. The 4.63 kJ $mol^{-1}$ destabilisation energy computed on progressing from ***XBDPP*** to **BDPP** arises from the interaction between one of the fluorine atoms and the para-phenyl hydrogen atoms of the benzyl groups which are separated by a distance slightly larger than the sum of their van der Waals radii[28] (2.97 vs 2.90 Å[23]). Dimer pair IV instead was observed to be stabilised by the sum of the following intermolecular interactions: T-shape interactions between one of the phenyl rings attached to the DPP core and the phenyl ring within one of the benzyl groups and the methylene hydrogen with the benzylic phenyl ring

as well as an H-bonding interaction between the ortho-phenylic hydrogen of the phenyl rings attached to the core and the electronegative carbonyl oxygen at 2.64 Å.

Analysis of the dimer pairs of ***THFBDPP*** revealed that pair I is stabilised by additive attractive interatomic interactions between the electronegative trifluoromethyl fluorine atoms and the electropositive ortho- and meta-phenylic hydrogens separated by distances of 2.59 and 3.02 Å respectively. The origin of the sole fluoro-benzyl induced stabilisation is established by analysis of the computed $\Delta E_{CP}$ for **BDPP** and **DPP** ($\Delta E_{CP}$ = -3.92 and -0.88 kJ mol$^{-1}$ respectively) which we associate to an intermolecular interaction between the electronegative meta-fluorine atom and the electropositive meta-hydrogen atom at 2.83 Å. The novel π-π stacking dimer pair II of ***THFBDPP*** is primarily stabilised by a strong cofacial interaction between the DPP cores and attached phenyl rings as extracted from the computed $\Delta E_{CP}$ of the associated **DPP** dimer pair ($\Delta E_{CP}$ = -127.55 and -97.32 kJ mol$^{-1}$ for ***XBDPP*** and **DPP** respectively). Nonetheless, significant additional stabilisation arises from benzyl/fluorine substitution. In short, a destabilisation of 22.78 kJ mol$^{-1}$ on removal of the benzyl groups was computed and associated to four identical intermolecular H-bonding interactions between the carbonyl oxygen and one of the electropositive methylene hydrogens separated by 2.61 Å. Negligible trifluoromethyl induced stabilisation was observed for the dimer pair III given the dimer symmetry (see Figure 14). In turn, large destabilisation was computed on progression from **BDPP** to **DPP** ($\Delta E_{CP}$ = -40.02 and -11.59 kJ mol$^{-1}$ respectively) attributed to methylene hydrogen-carboxylic oxygen H-bonding intermolecular interactions where the atoms are separated by 2.80 Å. Lastly, dimer pair IV of ***THFBDPP*** exhibits only benzyl induced stabilisation ($\Delta E_{CP}$ = -0.26 and -0.02 kJ mol$^{-1}$ for

**XDPP** and **DPP** respectively). We attribute the latter to distant dipole-dipole intermolecular interactions between the trifluoromethyl group and fluorinated benzylic phenyl rings.

Accordingly, via the detailed analysis of all the nearest neighbours extracted from the various investigated DPP systems we can conclude that, although weak, intermolecular F---H interactions involving organic fluorine play a significant role in stabilising these dimer pairs and therefore in determining their crystal structures. Despite the short intermolecular F---F contacts observed in these systems (such as in dimer pair I of ***HFHBDPP*** and dimer pairs II and III of ***HFFBDPP***), we propose that no attractive F---F intermolecular interactions are responsible for holding these dimer pairs together, which is entirely consistent with fluorine atoms unlike other halogen atoms exhibiting more F---H than F---F attractive intermolecular interactions.[23]

Lastly, given our interest in the development of organic conjugated DPP based materials to be employed as charge transfer mediators in optoelectronic devices, we computed the hole ($t_h$) and electron ($t_e$) transfer integrals for the centrosymmetric π-π dimer pairs of ***HFHBDPP*** and ***HFFBDPP*** within the framework of the energy splitting in dimer method[48] where $t_h/t_e$ is given by half the splitting between the dimer HOMO/HOMO(-1) and LUMO/LUMO(+1) orbitals. Computed charge transfer integrals for the dimer pair IV of ***HFHBDPP*** (0.50 and 3.68 kJ $mol^{-1}$ for $t_h$ and $t_e$ respectively) reveal $t_e > t_h$, consistent with our previously reported model system[20] for the slipped cofacial dimer pair of a non-substituted DPP (with computed values of $t_h$ = 3.01 and $t_e$ = 10.89 for a displacement $\Delta x$ = 3.6 Å). We attribute the significant lowering of the magnitude (but not sign) of both charge transfer integrals in the fluorinated system to the torsion of the phenyl rings attached to the core in ***HFHBDPP*** ($\theta$ = 38.23° as opposed to the fully planar

monomers in the model system) and the slightly increased vertical displacement of the monomers to from ca. Δz = 3.6 Å to 3.9 Å, diminishing the effective wavefunction overlap required for optimal electronic coupling.

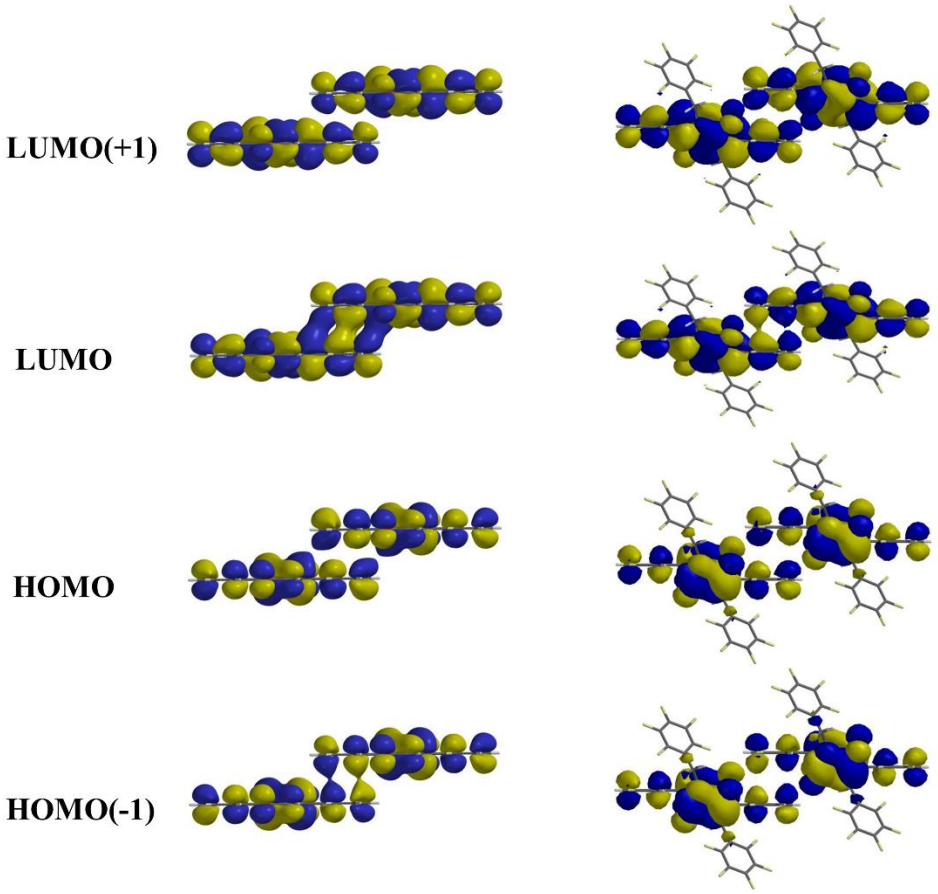


**Figure 15**. Kohn-Sham molecular orbitals of a model dimer system (left) for Δx = 9.0 Å and ***HFFBDPP*** (right). M06-2X/6-311G(d). IsoVal = 0.01.

In turn, a reversal of the trends predicted by the model system[20] ($t_h$ = 1.01 < $t_e$ = 5.33 kJ mol$^{-1}$ at Δx = 9.0 Å) was observed for the optimal sign of the computed charge transfer integrals of the π-π dimer pair of ***HFFBDPP*** (2.01 and 0.89 kJ mol$^{-1}$ for $t_h$ and $t_e$ respectively). We attribute this observation to the increased torsion of the phenyl rings in ***HFFBDPP*** (θ = 30.43°) as well as the

larger intermonomer displacement along the short molecular axis of this dimer, again lowering the effective wavefunction overlap. The decrease in magnitude of the electron transfer integral on progression from our previously reported model system (at $\Delta x = 9.0$ Å) to ***HFFBDPP*** ($t_e$ = 5.33 and 0.89 kJ $mol^{-1}$ respectively) can be further rationalised by considering the dimer wavefunction overlap. As illustrated in Figure 15, both gerade and ungerade LUMO(+1) orbitals of ***HFFBDPP*** and the model dimer pair exhibit weak anti-bonding character. As a consequence, the observed differences in computed electron transfer integrals ought to be related to the bonding/anti-bonding character of their LUMO orbitals. Whereas the computed gerade LUMO of the model dimer exhibits large wavefunction overlap and strong bonding character, the ungerade LUMO of ***HFFBDPP*** is characterised by a weak bonding interaction. The variation in computed charge transfer integrals is therefore entirely consistent with the bonding/anti-bonding character of the associated molecular orbitals in these dimers. For the systems reported herein, it is clearly apparent that direct fluorination of the DPP core phenyl rings and benzyl substituents plays a significant role in defining the predicted sign of charge carrier and may actually be detrimental to the charge transport behaviour in these single crystal structures.

## CONCLUSIONS

In conclusion, four novel fluorinated DPP based systems and their single crystal structures have been reported and studied in detail. The structures involving direct fluorination of the DPP core phenyl rings and benzyl groups, ***HFHBDPP*** and ***HFFBDPP*** display 1-dimensional π-π stacking motifs which are a characteristic of N-benzyl substitution, with the degree of long and short molecular axis displacement induced by isosteric substitution of the phenylic hydrogen atoms for fluorine atoms within the benzyl groups. The characteristic stacking behaviour observed in those

structures is however collapsed upon trifluoromethyl substitution at the para position of the phenyl rings in both ***THHBDPP*** and ***THFBDPP***. A novel molecular conformation and π-π dimer pair was identified for the latter structure, demonstrating a higher computed intermolecular interaction energy than any other structurally analogous DPP based system reported previously. Furthermore, the single crystal structure of ***THFBDPP*** also exhibits a unique orthogonal association of these π-π dimer pairs along the crystallographic *a* and *b* axes, resulting in the formation of a framework that is characterised by well-defined channels perpetuating along the length of the crystallographic *c* axis. The role of substituent induced stabilisation in each of the structures was investigated in detail via analysis of the computed intermolecular interactions for all the nearest neighbour dimer pairs and their associated cropped equivalents. The impact of organic fluorine induced stabilisation is clearly observed in various types of weak additive intermolecular interactions, such as C-F---H, C-F---$\pi_F$ and C-F---π. Little evidence of C-F---F-C stabilising intermolecular interactions were observed, which is in line with other reported analyses involving organic fluorine. Finally, charge transfer integrals were computed for the centrosymmetric π-π dimer pairs of ***HFHBDPP*** and ***HFFBDPP***. A $t_e > t_h$ transfer integral was computed for ***HFHBDPP***, which is in agreement with our previously reported model system. The diminished magnitude of the predicted integral is directly related to fluorination of the DPP core phenyl rings, resulting in an increased torsion of the phenyl rings and increased intermonomer Δz displacement. Upon additional benzyl fluorination in ***HFFBDPP*** $t_h > t_e$ was computed, which is contrary to the trend predicted by our model system and is attributed to the larger displacement along the short molecular axis and changes to the bonding/anti-bonding character of the associated supramolecular orbitals in this case. In summary, these results clearly reinforce our previous assertion of the positive role of benzyl substitution in DPPs crystal

structures to enhance optoelectronic behaviour. More importantly however, they demonstrate the significant impact small changes in molecular structure can have on the solid state properties of this molecular motif, particularly when fluorination is involved. As a consequence and given the significant current interest in the use of organic fluorine to manipulate electrochemical behaviour in organic semiconductors and influence their solid state packing we believe that this study should be of value to those engaged in the rational understanding of intermolecular interactions in organic conjugated systems, and in particular to those interested in the optoelectronic application of DPP single crystals.

## SUPPORTING INFORMATION

Number of equivalent molecules and site for all nearest neighbour dimer pairs of ***XYZBDPP***s. X-ray crystallographic information files (CIF) are available free of charge via the Internet at http://pubs.acs.org. Crystallographic information files are also available from the Cambridge Crystallographic Data Centre (CCDC) upon request (http://www.ccdc.ca.ac.uk), CCDC deposition numbers 1449852-1449855.

## AUTHOR INFORMATION

### Corresponding Authors

*E-mail: callum.mchugh@uws.ac.uk

*E-mail: j.calvo-castro@herts.ac.uk

### Notes

The authors declare no competing financial interest.

## ACKNOWLEDGMENT

C.J.M acknowledges the EPSRC for funding under the First Grant Scheme (EP/J011746/1) and the University of the West of Scotland for Ph.D. funding for G.M. and research funding for J.C-C.

## REFERENCES

(1) Wallquist, O.; Lenz, R. *Macromol. Symp.* **2002**, *187*, 617.
(2) Hao, Z. M.; Iqbal, A. *Chem. Soc. Rev.* **1997**, *26*, 203.
(3) Christie, R. M. *Colour Chemistry*; The Royal Society of Chemistry, 2001.
(4) Herbst, W.; Hunger, K. *Industrial Organic Pigments*; Wiley-VCH, 2004.
(5) Smith, H. M. *High Performance Pigments*; Wiley-VCH, 2002.
(6) Qu, S.; Qin, C.; Islam, A.; Wu, Y.; Zhu, W.; Hua, J.; Tian, H.; Han, L. *Chem. Commun.* **2012**, *48*, 6972.
(7) Qu, S.; Tian, H. *Chem. Commun.* **2012**, *48*, 3039.
(8) Qu, S.; Wu, W.; Hua, J.; Kong, C.; Long, Y.; Tian, H. *J. Phys. Chem. C* **2010**, *114*, 1343.
(9) Guo, X.; Puniredd, S. R.; He, B.; Marszalek, T.; Baumgarten, M.; Pisula, W.; Muellen, K. *Chem. Mater.* **2014**, *26*, 3595.
(10) Bronstein, H.; Chen, Z.; Ashraf, R. S.; Zhang, W.; Du, J.; Durrant, J. R.; Tuladhar, P. S.; Song, K.; Watkins, S. E.; Geerts, Y.; Wienk, M. M.; Janssen, R. A. J.; Anthopoulos, T.; Sirringhaus, H.; Heeney, M.; McCulloch, I. *J. Am. Chem. Soc.* **2011**, *133*, 3272.
(11) Liu, J.; Sun, Y.; Moonsin, P.; Kuik, M.; Proctor, C. M.; Lin, J.; Hsu, B. B.; Promarak, V.; Heeger, A. J.; Thuc-Quyen, N. *Adv. Mater.* **2013**, *25*, 5898.
(12) Hong, W.; Sun, B.; Aziz, H.; Park, W.-T.; Noh, Y.-Y.; Li, Y. *Chem. Commun.* **2012**, *48*, 8413.
(13) Lee, J.; Cho, S.; Seo, J. H.; Anant, P.; Jacob, J.; Yang, C. *J. Mater. Chem.* **2012**, *22*, 1504.
(14) Chen, Z.; Lee, M. J.; Ashraf, R. S.; Gu, Y.; Albert-Seifried, S.; Nielsen, M. M.; Schroeder, B.; Anthopoulos, T. D.; Heeney, M.; McCulloch, I.; Sirringhaus, H. *Adv. Mater.* **2012**, *24*, 647.

(15) Cortizo-Lacalle, D.; Arumugam, S.; Elmasly, S. E. T.; Kanibolotsky, A. L.; Findlay, N. J.; Inigo, A. R.; Skabara, P. J. *J. Mater. Chem.* **2012**, *22*, 11310.

(16) Ha, J. S.; Kim, K. H.; Choi, D. H. *J. Am. Chem. Soc.* **2011**, *133*, 10364.

(17) Sonar, P.; Singh, S. P.; Li, Y.; Soh, M. S.; Dodabalapur, A. *Adv. Mater.* **2010**, *22*, 5409.

(18) Warzecha, M.; Calvo-Castro, J.; Kennedy, A. R.; Macpherson, A. N.; Shankland, K.; Shankland, N.; McLean, A. J.; McHugh, C. J. *Chem. Commun.* **2015**, *51*, 1143.

(19) Calvo-Castro, J.; Warzecha, M.; Kennedy, A. R.; McHugh, C. J.; McLean, A. J. *Cryst. Growth Des.* **2014**, *14*, 4849.

(20) Calvo-Castro, J.; Warzecha, M.; Oswald, I. D. H.; Kennedy, A. R.; Morris, G.; McLean, A. J.; McHugh, C. J. *Cryst. Growth Des.* **2016**.

(21) Coropceanu, V.; Cornil, J.; da Silva Filho, D. A.; Olivier, Y.; Silbey, R.; Bredas, J.-L. *Chem. Rev.* **2007**, *107*, 926.

(22) Bredas, J. L.; Calbert, J. P.; da Silva, D. A.; Cornil, J. *Proc. Natl. Acad. Sci.U.S.A* **2002**, *99*, 5804.

(23) Reichenbacher, K.; Suss, H. I.; Hulliger, J. *Chem. Soc. Rev.* **2005**, *34*, 22.

(24) Dunitz, J. D.; Taylor, R. *Chem. Eur. J.* **1997**, *3*, 89.

(25) Dunitz, J. D. *Chembiochem* **2004**, *5*, 614.

(26) Nayak, S. K.; Reddy, M. K.; Row, T. N. G.; Chopra, D. *Cryst. Growth Des.* **2011**, *11*, 1578.

(27) Chopra, D.; Row, T. N. G. *CrystEngComm* **2011**, *13*, 2175.

(28) Berger, R.; Resnati, G.; Metrangolo, P.; Weber, E.; Hulliger, J. *Chem. Soc. Rev.* **2011**, *40*, 3496.

(29) Wang, C.; Dong, H.; Hu, W.; Liu, Y.; Zhu, D. *Chem. Rev.* **2012**, *112*, 2208.

(30) Yin, Q.-R.; Miao, J.-S.; Wu, Z.; Chang, Z.-F.; Wang, J.-L.; Wu, H.-B.; Cao, Y. *J. Mater. Chem. A* **2015**, *3*, 11575.

(31) Wang, J.-L.; Chang, Z.-F.; Song, X.-X.; Liu, K.-K.; Jing, L.-M. *J. Mat. Chem. C* **2015**, *3*, 9849.

(32) Wang, Y.; Huang, Q.; Liu, Z.; Li, H. *RSC Adv.* **2014**, *4*, 29509.

(33) Sheldrick, G. M. *Acta Crystallogr. Sect. A* **2008**, *64*, 112.

(34) Shao, Y.; Molnar, L. F.; Jung, Y.; Kussmann, J.; Ochsenfeld, C.; Brown, S. T.; Gilbert, A. T. B.; Slipchenko, L. V.; Levchenko, S. V.; O'Neill, D. P.; DiStasio, R. A., Jr.; Lochan, R. C.; Wang, T.; Beran, G. J. O.; Besley, N. A.; Herbert, J. M.; Lin, C. Y.; Van Voorhis, T.; Chien, S. H.; Sodt, A.; Steele, R. P.; Rassolov, V. A.; Maslen, P. E.; Korambath, P. P.; Adamson, R. D.; Austin, B.; Baker, J.; Byrd, E. F. C.; Dachsel, H.; Doerksen, R. J.; Dreuw, A.; Dunietz, B. D.; Dutoi, A. D.; Furlani, T. R.; Gwaltney, S. R.; Heyden, A.; Hirata, S.; Hsu, C.-P.; Kedziora, G.; Khalliulin, R. Z.; Klunzinger, P.; Lee, A. M.; Lee, M. S.; Liang, W.; Lotan, I.; Nair, N.; Peters, B.; Proynov, E. I.; Pieniazek, P. A.; Rhee, Y. M.; Ritchie, J.; Rosta, E.; Sherrill, C. D.; Simmonett, A. C.; Subotnik, J. E.; Woodcock, H. L., III; Zhang, W.; Bell, A. T.; Chakraborty, A. K.; Chipman, D. M.; Keil, F. J.; Warshel, A.; Hehre, W. J.; Schaefer, H. F., III; Kong, J.; Krylov, A. I.; Gill, P. M. W.; Head-Gordon, M. *Phys. Chem. Chem. Phys.* **2006**, *8*, 3172.

(35) Boys, S. F.; Bernardi, F. *Mol. Phys.* **2002**, *100*, 65.

(36) Zhao, Y.; Truhlar, D. G. *Theor. Chem. Acc.* **2008**, *120*, 215.

(37) Wheeler, S. E.; McNeil, A. J.; Müller, P.; Swager, T. M.; Houk, K. N. *J. Am. Chem. Soc.* **2010**, *132*, 3304.

(38) Vura-Weis, J.; Ratner, M. A.; Wasielewski, M. R. *J. Am. Chem. Soc.* **2010**, *132*, 1738.
(39) Mizuguchi, J.; Miyazaki, T. *Z.Krist-New Cryst. St.* **2002**, *217*, 43.
(40) Mizuguchi, J.; Grubenmann, A.; Rihs, G. *Acta Crystallogr. Sect. B* **1993**, *49*, 1056.
(41) Mizuguchi, J.; Grubenmann, A.; Wooden, G.; Rihs, G. *Acta Crystallogr. Sect. B* **1992**, *48*, 696.
(42) Mas-Torrent, M.; Rovira, C. *Chem. Rev.* **2011**, *111*, 4833.
(43) Reese, C.; Roberts, M. E.; Parkin, S. R.; Bao, Z. *Adv. Mater.* **2009**, *21*, 3678.
(44) Curtis, M. D.; Cao, J.; Kampf, J. W. *J. Am. Chem. Soc.* **2004**, *126*, 4318.
(45) da Silva, D. A.; Kim, E. G.; Bredas, J. L. *Adv. Mater.* **2005**, *17*, 1072.
(46) McGarry, K. A.; Xie, W.; Sutton, C.; Risko, C.; Wu, Y.; Young, V. G., Jr.; Bredas, J.-L.; Frisbie, C. D.; Douglas, C. J. *Chem. Mater.* **2013**, *25*, 2254.
(47) Podzorov, V.; Menard, E.; Borissov, A.; Kiryukhin, V.; Rogers, J. A.; Gershenson, M. E. *Phys. Rev. Lett.* **2004**, *93*.
(48) Bredas, J. L.; Beljonne, D.; Coropceanu, V.; Cornil, J. *Chem. Rev.* **2004**, *104*, 4971.
(49) Wheeler, S. E. *Acc. Chem. Res.* **2013**, *46*, 1029.
(50) Wheeler, S. E.; Bloom, J. W. G. *J. Phys. Chem. A* **2014**, *118*, 6133.
(51) Tauer, T. P.; Sherrill, C. D. *J. Phys. Chem. A* **2005**, *109*, 10475.
(52) Sinnokrot, M. O.; Sherrill, C. D. *J. Am. Chem. Soc.* **2004**, *126*, 7690.
(53) Parrish, R. M.; Parker, T. M.; Sherrill, C. D. *J. Chem. Theory Comput.* **2014**, *10*, 4417.
(54) Burns, L. A.; Marshall, M. S.; Sherrill, C. D. *J. Chem. Theory Comput.* **2014**, *10*, 49.
(55) Hohenstein, E. G.; Chill, S. T.; Sherrill, C. D. *J. Chem. Theory Comput.* **2008**, *4*, 1996.
(56) Antony, J.; Alameddine, B.; Jenny, T. A.; Grimme, S. *J. Phys. Chem. A* **2013**, *117*, 616.
(57) Grimme, S. *Angewandte Chemie-International Edition* **2008**, *47*, 3430.
(58) Wheeler, S. E.; Houk, K. N. *J. Am. Chem. Soc.* **2008**, *130*, 10854.
(59) Wheeler, S. E.; Houk, K. N. *J. Chem. Theory Comput.* **2009**, *5*, 2301.
(60) Raju, R. K.; Bloom, J. W. G.; An, Y.; Wheeler, S. E. *Chemphyschem* **2011**, *12*, 3116.
(61) Wheeler, S. E. *CrystEngComm* **2012**, *14*, 6140.
(62) Parrish, R. M.; Sherrill, C. D. *J. Am. Chem. Soc.* **2014**, *136*, 17386.
(63) Sherrill, C. D. *Acc. Chem. Res.* **2013**, *46*, 1020.
(64) Sinnokrot, M. O.; Sherrill, C. D. *J. Phys. Chem. A* **2004**, *108*, 10200.
(65) Cozzi, F.; Ponzini, F.; Annunziata, R.; Cinquini, M.; Siegel, J. S. *Angew. Chem. Int. Ed. Engl.* **1995**, *34*, 1019.
(66) Howard, J. A. K.; Hoy, V. J.; Ohagan, D.; Smith, G. T. *Tetrahedron* **1996**, *52*, 12613.
(67) Shimoni, L.; Glusker, J. P. *Struct. Chem.* **1994**, *5*, 383.

**For Table of Contents Use Only**

**Effects of fluorine substitution on the intermolecular interactions, energetics and packing behaviour of N-benzyl substituted diketopyrrolopyrroles**

*Jesus Calvo-Castro,*[c] Graeme Morris,[a] Alan R. Kennedy,[b] and Callum J. McHugh*[a]*

[a] *School of Science and Sport, University of the West of Scotland, Paisley, PA1 2BE, UK.*
[b] *Department of Pure & Applied Chemistry, University of Strathclyde, Glasgow, G1 1XL, UK.*
[c] *School of Life and Medical Sciences, University of Hertfordshire, Hatfield, AL10 9AB, UK.*

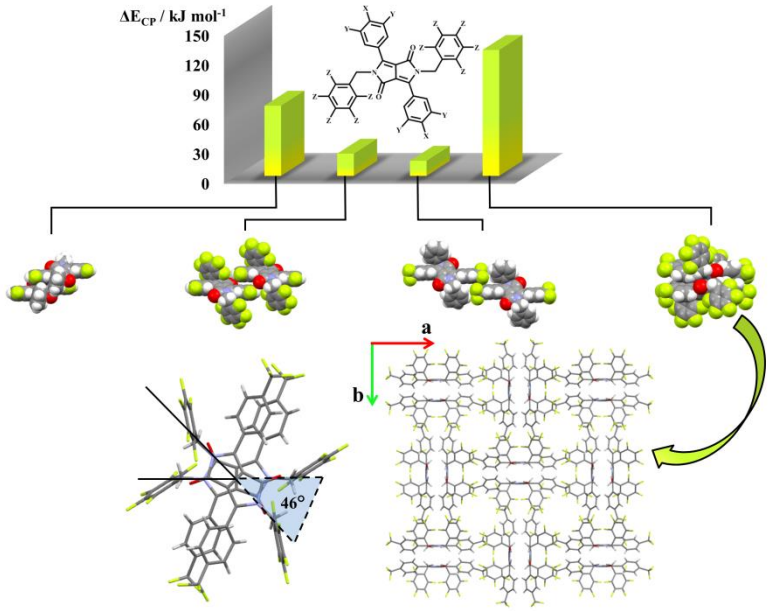


A series of novel systematically fluorinated N-benzyl diketopyrrolopyrrole crystal structures are reported. The impact of small changes in molecular structure on the solid state properties of this molecular motif and the emergence of significant fluorine induced stabilisation were clearly identified, computed and rationalised through a comprehensive analysis of those intermolecular interactions extracted from the single crystal nearest neighbour dimer pairs.